

# Ni-catalyzed ligand-controlled divergent and selective synthesis

Yang Ke, Wei Li, Wenfeng Liu &amp; Wangqing Kong\*

*The Institute for Advanced Studies (IAS), Wuhan University, Wuhan 430072, China*

Received January 10, 2023; accepted February 2, 2023; published online May 5, 2023

Scaffold diversity is a key feature of a compound library and plays a pivotal role in its success in biological screening. Therefore, it is highly desirable to develop efficient strategies to rapidly construct structurally distinct and diverse “privileged” molecular scaffolds, thereby giving rise to compound libraries with selective and differing biological activities. This review covers recent efforts in this emerging field of Ni-catalyzed divergent and selective synthesis, and will focus on reactions using the same substrate to generate structurally diverse molecular scaffolds by varying the ligand backbone under otherwise almost identical reaction conditions. We hope that the field will be encouraged by the progress achieved, drawing attention to the design and development of new selective catalytic systems, and revealing new modes of catalytic transformation for broader synthetic applications.

**nickel catalysis, chemoselectivity, regioselectivity, stereoselectivity, divergent synthesis**

**Citation:** Ke Y, Li W, Liu W, Kong W. Ni-catalyzed ligand-controlled divergent and selective synthesis. *Sci China Chem*, 2023, 66: 2951–2976, <https://doi.org/10.1007/s11426-023-1533-y>

## 1 Introduction

The art of organic synthesis provides chemists with a powerful toolbox for creating new molecules with novel properties. Small molecule drugs are often discovered through high-throughput screening of compound libraries [1,2]. However, some human disease-related targets could not be addressed by commonly used compound libraries, which mainly consist of a large number of structurally similar molecules. Scaffolds are considered as the core structures of compounds, determining their shape, rigidity, and flexibility [3], and placing functional moieties in the correct sites to interact with biological targets. Therefore, scaffold diversity is a key feature of a compound library and determines its success in screening efforts [4–8], especially when identifying bioactive molecules in unbiased phenotypic screenings, where rational ligand design is very difficult. Molecule libraries rich in scaffold diversity are more likely to identify

hit and lead compounds. As a result, there has been a paradigm shift in library construction over the past decade, with a particular emphasis now being placed on increasing the diversity and complexity of the library’s core scaffolds, rather than just its size.

In the conventional methods for synthesizing structurally diverse molecular scaffolds, the starting materials are usually varied in structure and subjected to transformation by different reagents and catalysts under individually established reaction conditions, which renders them time-consuming and laborious. In transition metal-catalyzed reactions, the activity and selectivity of metal complex catalysts can be tuned by modifying the electronic and steric properties of the ligands. Specifically, common starting materials are exposed to a common mode of catalysis, and ligands around the metal center can modulate the reaction pathways to form structurally diverse scaffolds. Therefore, the ligand-directed divergent synthesis strategy has attracted more and more attention [9–17]. This strategy not only provides facile and efficient access to structurally rich compound libraries,

\*Corresponding author (email: [wqkong@whu.edu.cn](mailto:wqkong@whu.edu.cn))

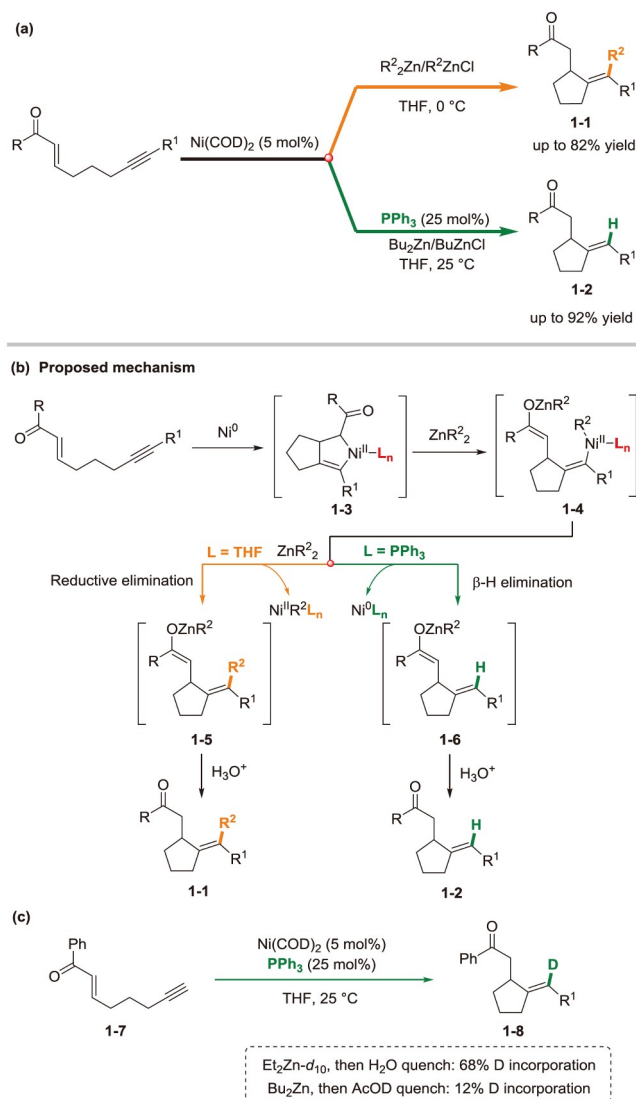
which in turn can offer small molecules with diverse and selective biological activities, but also reveals novel modes of catalytic transformations for broader synthetic applications.

In this review, we highlight recent achievements, which have led to intriguing transformations, and thus structurally diverse and interesting small molecules, in the emerging field of nickel-catalyzed divergent and selective synthesis. Under otherwise almost identical reaction conditions, the reaction pathways can be controlled by the ligands, thus leading to structurally diverse scaffolds. The following issues are discussed herein: (1) obtaining different products from common starting materials by fine-tuning the ligands to control chemoselectivity, regioselectivity, or stereoselectivity; and (2) understanding the reaction mechanisms with respect to the selectivities.

## 2 Chemoselectivity

The development of nickel-catalyzed multicomponent coupling processes involving an enone and an organozinc poses an interesting challenge in chemoselectivity since simple conjugate additions must be avoided. Studies from Montgomery *et al.* [18] and Ikeda and Sato *et al.* [19] independently demonstrated the three component coupling of enones, alkynes, and organozincs to generate products in which the organozinc was formally added to the alkyne, not to the enone. The Ni-catalyzed ligand-controlled divergent alkylation and reductive cyclization of alkynyl enones with organozinc reagents were reported by Montgomery *et al.* [18]. In the absence of ligand, aryl-, alkenyl-, and alkyl-substituted organozincs, including those bearing  $\beta$ -hydrogens, underwent alkylation cyclizations to yield  $\beta$ -alkenyl ketones **1-1** with complete control over the alkene geometry. When Ni(COD)<sub>2</sub> (COD = 1,5-cyclooctadiene) was pretreated with PPh<sub>3</sub>, an efficient reductive cyclization rather than alkylation cyclization occurred in the reaction involving di-butylzinc, resulting in a single isomer of the trisubstituted alkene **1-2**, with hydrogen always delivering *cis* to the ketone functionality (Scheme 1a).

A possible reaction mechanism was proposed in Scheme 1b. The reaction is initiated by the oxidative cyclization of alkynyl enones with Ni(0) species to afford the cyclic-Ni(II) intermediate **1-3**, which then undergoes transmetalation with organozinc reagents to deliver alkenyl-nickel intermediate **1-4**. **1-4** is a common intermediate in both reductive cyclization and alkylation cyclization pathways, which was confirmed by deuterium labeling experiments (Scheme 1c). In the presence of excess phosphine, the alkenyl-nickel intermediate **1-4** is substantially more electron-rich at nickel, and thus  $\beta$ -hydride elimination may be preferred over reductive elimination. In the absence of a phosphine ligand, the  $\pi$ -

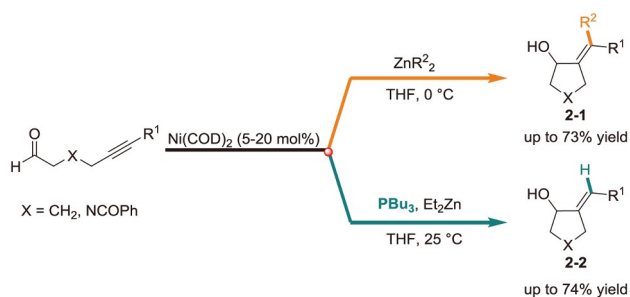


**Scheme 1** Ni-catalyzed ligand-controlled divergent alkylation and reductive cyclizations of alkynyl enones [18] (color online).

acceptor nature of the COD or THF (THF = tetrahydrofuran) ligand reduces the electron density at the nickel center, therefore facilitating the reductive elimination process by producing an electron-deficient Ni(II)  $\pi$ -complex.

Subsequently, the same group disclosed a similar Ni-catalyzed ligand-controlled divergent alkylation and reductive cyclization of ynals with organozincs for the highly regioselective and stereoselective synthesis of allylic alcohols with tri- and tetrasubstituted alkenes [20]. In the absence of phosphine ligands, both  $sp^2$ - and  $sp^3$ -hybridized organozincs, including those that possess  $\beta$ -hydrogens, were efficiently incorporated without competing  $\beta$ -hydride elimination. Alternatively, selective reductive cyclization with both terminal and internal alkynes was observed simply by pretreating the Ni(COD)<sub>2</sub> with PBu<sub>3</sub> (Scheme 2).

Compounds containing allyl moieties are widely found in natural products and bioactive molecules, and are often used



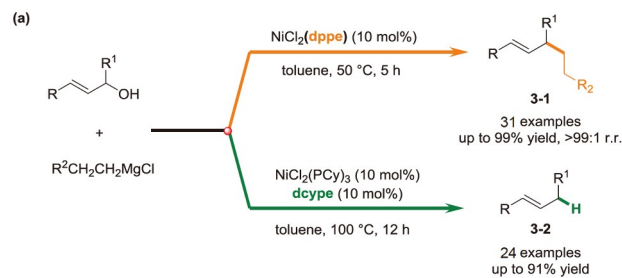
**Scheme 2** Ni-catalyzed ligand-controlled divergent alkylation and reductive cyclizations of ynals [20] (color online).

as versatile building blocks in organic synthesis. Therefore, the synthesis and transformation of allyl compounds have attracted much attention. In 2020, Wang *et al.* [21] reported a Ni-catalyzed ligand-controlled selective alkylation or reduction of allylic alcohols with alkyl Grignard reagents. The reaction using Ni(dppe)Cl<sub>2</sub> as a catalyst resulted in the ipso-coupling of allylic alcohols with primary alkyl Grignard reagents, including  $\beta$ -H-containing and  $\beta$ -H-free ones, as well as the secondary alkyl Grignard reagents. The combination of dcype and Ni(PCy<sub>3</sub>)<sub>2</sub>Cl<sub>2</sub> led to the reduction of allylic alcohols by primary, secondary, and tertiary alkyl Grignard reagents (Scheme 3a). A range of allylic alcohols, including 3-aryl and 3-alkyl allylic alcohols, 1,3-disubstituted allylic alcohols, and 1-aryl allylic alcohols, can be used in the coupling or reductive reactions.

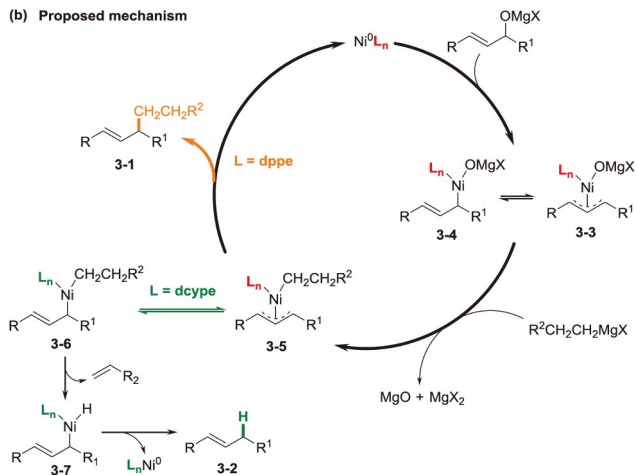
A possible reaction mechanism involving Ni(0)/Ni(II) process was proposed in Scheme 3b. Oxidative addition of Ni(0) with allyloxomagnesium will afford Ni(II)-allyl intermediate, including  $\eta^3$ -allyl-Ni(II) **3-3** and  $\eta^1$ -allyl-Ni(II) **3-4** species as an equilibrium mixture. Transmetalation of **3-3** and **3-4** with the Grignard reagent forms allyl-nickel complexes **3-5** ( $\eta^3$ -allyl) and **3-6** ( $\eta^1$ -allyl) as another equilibrium mixture. In the presence of bulky and electron-rich ligand (dcype),  $\eta^1$ -allyl-Ni(II)-alkyl species **3-4** and **3-6** will dominate the equilibrium, which favors the  $\beta$ -H elimination process to afford the product **3-2**. When the ligand is not bulky enough (dppe),  $\eta^3$ -allyl-nickel **3-3** and **3-5** may be the main components in the respective equilibrium. Reductive elimination of **3-5** results in  $\alpha$ -alkylated product of the allyl alcohol **3-1**.

Montgomery and co-workers [22] developed nickel-catalyzed selective reductive cycloadditions or alkylation couplings of enals and alkynes using triethyl borane as the reducing agent. The use of bulky P(*o*-tol)<sub>3</sub> as a ligand favored the generation of the alkylation coupling products **4-1**. Alternatively, the use of a stable triarylphosphine ligand TTMPP (**L1**) favored the formation of [3+2] reductive cycloaddition products **4-2**, providing a useful preparative simplification compared with previously reported use of PBU<sub>3</sub> (Scheme 4a).

A plausible mechanism was depicted in Scheme 4b. Oxi-



**(b) Proposed mechanism**

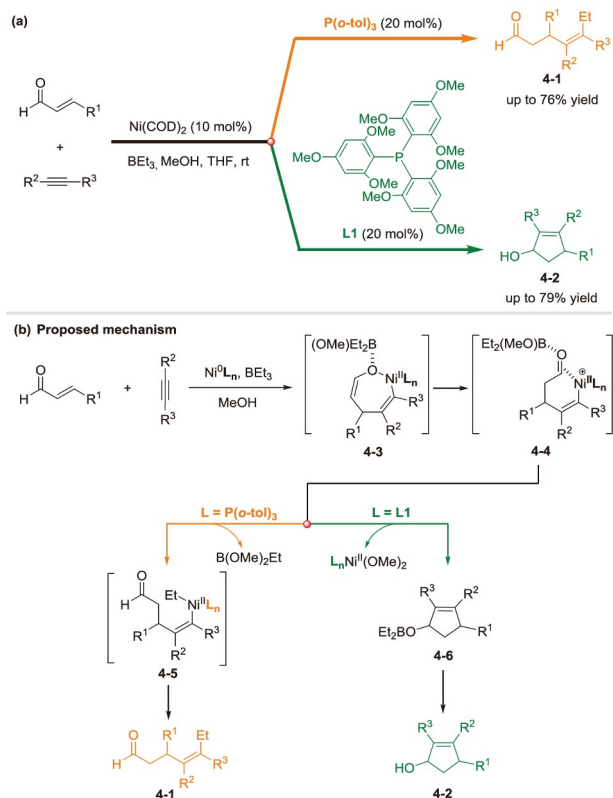


**Scheme 3** Ni-catalyzed ligand-controlled divergent alkylation or reduction of allylic alcohols with alkyl Grignard reagents [21] (color online).

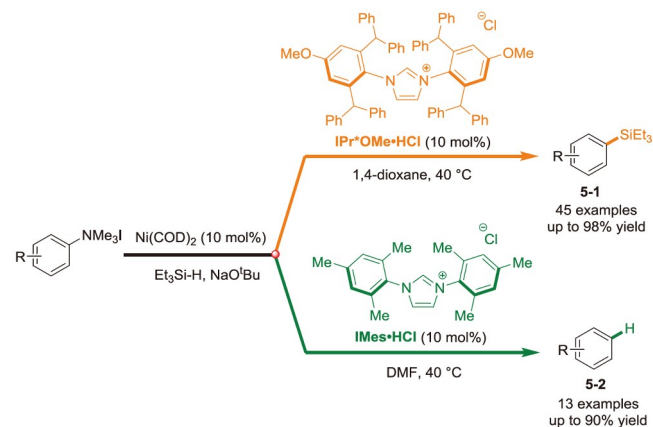
ductive cyclometallation of enals and alkynes produces metallacycle intermediate **4-3** that can be protonated to give the common alkenyl-Ni(II) intermediate **4-4**. The use of electron-donating phosphine ligands (PBU<sub>3</sub> or TTMPP) allows the direct addition of vinylnickel species to the coordinated aldehyde of **4-4**, while electronically disfavoring the ethyl group transfer to **4-5** because of the strong  $\sigma$ -donor capability of these ligands. Thus, this addition leads to the cyclopentenol **4-2** as the major product. In contrast, the use of less basic arylphosphines as ligands will facilitate ethyl transfer and further reductive elimination to yield alkylation couplings product **4-1**.

In 2017, Montgomery *et al.* [23] disclosed a Ni-catalyzed direct conversion of C(sp<sup>2</sup>)-O bond of arylsilyl ethers into C-H or C-Si bonds using Ti(*o*-i-Pr)<sub>4</sub> or trialkylsilanes as reagents. Subsequently, the same group developed a Ni-catalyzed ligand-controlled selective reduction or silylation of aryl trialkylammonium salts to arenes or aryl silanes [24]. The silylation/reduction selectivity was controlled through the size of NHC ligand. The use of a large NHC (IPr\*O-Me•HCl) produces aryl silanes. Alternatively, a small NHC (IMes•HCl) promotes reduction to arenes (Scheme 5). This method provided a streamlined approach to high-value aryl silanes, starting from commercially available nitro- and aniline-containing compounds.

Ong *et al.* [25] disclosed a Ni-catalyzed ligand-controlled hydroheteroarylation of cyclic dienes *via* C-H bond activa-



**Scheme 4** Ni-catalyzed couplings of enals and alkynes [22] (color online).

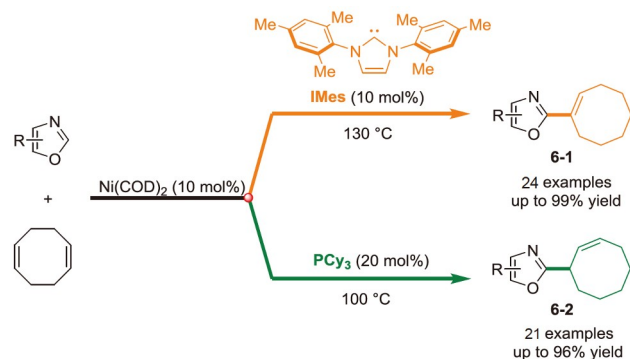


**Scheme 5** Ni-catalyzed reduction and silylation of aryl trialkylammonium salts [24] (color online).

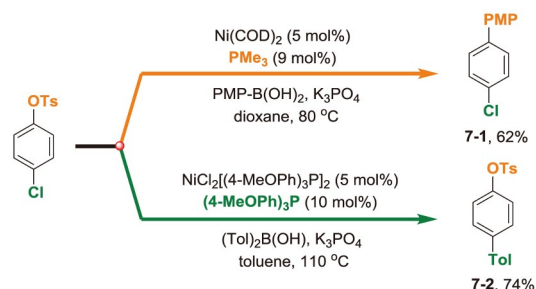
tion of heteroarenes. Hydroheteroarylation of cyclic dienes with azoles in the presence of N-heterocyclic carbene (IMes) ligand led to Heck-like product  $\alpha$ -alkenyl-azoles **6-1**. In contrast, changing the ligand to PCy<sub>3</sub> switched this reaction pathway to afford isomeric  $\beta$ -alkenyl-substituted azoles **6-2** (Scheme 6). This ligand-controlled divergent synthesis mechanism is due to the rapid conversion of product **6-2** to the more stable isomer **6-1** when using the Ni(0)/IMes catalyst. However, the conversion of **6-2** to **6-1** was very slow in the presence of Ni(COD)<sub>2</sub> and PCy<sub>3</sub>.

Although nickel-catalyzed cross-coupling of phenol derivatives has been established, a key limitation of current methods is the incompatibility of aryl halides such as chlorides. This is due to the tendency of organohalides to undergo oxidative addition to Ni(0) at a rate similar to or faster than that of the Ar–O bond. Therefore, the nickel-catalyzed selective cross-coupling of chlorophenol derivatives is extremely challenging. In 2014, Zou *et al.* [26] developed a nickel/triarylphosphine catalyst system for the chemical selective cross-coupling of C<sub>Ar</sub>–Cl of chlorophenol tosylates and bis(*p*-tolyl)boronic acid. Subsequently, Neufeldt and co-workers [27] further realized a Ni-catalyzed chemoselective Suzuki–Miyaura coupling of C<sub>Ar</sub>–OTs of chlorophenol tosylates with 4-methoxyphenylboronic acid by using PMe<sub>3</sub> as a ligand (Scheme 7). Density functional theory (DFT) calculations revealed that small phosphines are uniquely advantageous in promoting the reaction of Ni(COD)<sub>2</sub> with C<sub>Ar</sub>–OTs of chlorophenol tosylates, particularly PMe<sub>3</sub>, for its electronic and steric effects.

Transition metal-catalyzed coupling reactions of alkynes have demonstrated important synthetic utility in the preparation of enynes, which are versatile building blocks in organic synthesis. Miura *et al.* [28] reported a nickel-catalyzed ligand-controlled cross-dimerization and -trimerization of diphenylacetylene with trimethylsilylacetylene *via* C–H bond cleavage. In the presence of a pyridine-based ligand (DMAP), the cross-dimerization reaction proceeded



**Scheme 6** Ni-catalyzed switchable hydroheteroarylation of cyclodienes [25] (color online).



**Scheme 7** Ni-catalyzed chemoselective Suzuki–Miyaura coupling of chlorophenol tosylate [26,27] (color online).

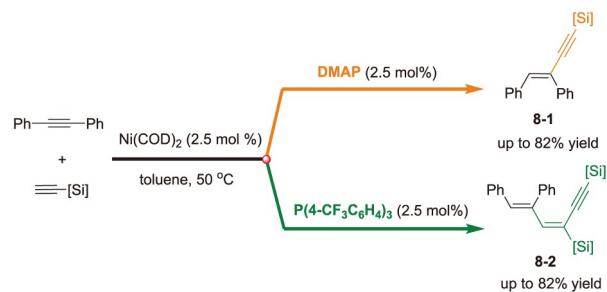
efficiently to give the corresponding enynes **8-1** in good yield. In contrast, when a phosphine ligand ( $\text{P}(\text{4-CF}_3\text{C}_6\text{H}_4)_3$ ) was used, a cross-trimerization reaction occurred selectively to give the diyne products **8-2** (Scheme 8).

Conjugated sulfur-containing molecules are of special demand in bio-, opto-, and alternative energy electronics due to their enhanced mechanical and optical properties and excellent charge conductivity. Ananikov *et al.* [29] reported a Ni-catalyzed switchable dithiolation of acetylene with aryl disulfides. The use of  $\text{PPh}_3$  as a ligand resulted in the selective formation of (*Z*)-1,2-bis(arylthio)ethenes **9-1**. Replacing  $\text{PPh}_3$  with  $\text{PPhCy}_2$  shifted the reaction towards the formation of (*Z,Z*)-1,4-bis(arylthio)buta-1,3-dienes **9-2** (Scheme 9a).

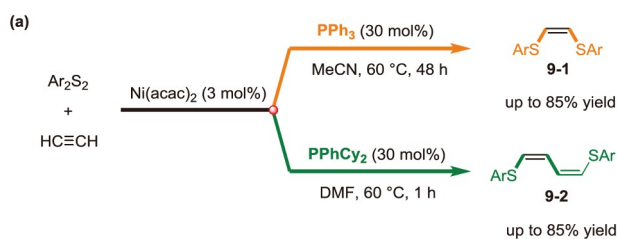
The strength of Ni–P bond in the nickel-phosphine complex with the more electron-donating  $\text{PPhCy}_2$  is higher than that in the complex with  $\text{PPh}_3$ . Moreover, the formation of solid  $[\text{Ni}(\text{SAr})_2]_n$  was observed for  $\text{PPh}_3$ , but not for  $\text{PPhCy}_2$ . In the case of a low electron-donating phosphine ligand ( $\text{PPh}_3$ ), intermediate **9-4** is more prone to undergo reductive elimination to give bis(arylthio)ethene **9-1**. However, for the more electron-donating  $\text{PPhCy}_2$ , the rate of the elimination step is lower, and thus the reaction proceeds through the insertion of a second alkyne into the Ni–C bond and leads to the formation of bis(arylthio)-1,3-butadiene **9-2**. The insertion mode of the second acetylene molecule and the structure of intermediate **9-5** were deduced from DFT calculation studies (Scheme 9b).

Recently, Zhao and co-workers [30] reported a nickel/copper dual-catalyzed divergent allylic alkynylation of vinyl epoxides using alkynes. Under otherwise identical reaction conditions, the use of a strong bisphosphine ligand (Xantphos) resulted in the formation of functionalized branched 1,4-enynes **10-1**. Alternatively, the use of hemilabile P,N-ligand (Me-PHOX) resulted in the formation of enyne-containing allyl alcohols and amines **10-2** (Scheme 10). DFT calculations showed that the activation barrier for the bisphosphine ligand dissociation pathway was determined to be much less favorable. However, alkyne coordination with the release of Me-PHOX ligand was considered to be energetically favorable. The hemilabile property of this P,N-ligand involved in dynamic association and dissociation is a key factor for this intriguing trimolecular reaction to take place.

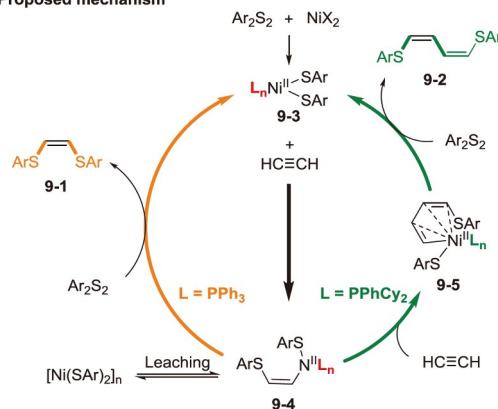
In 2018, Rueping and co-workers [31] demonstrated a Ni-catalyzed ligand-controlled and site-selective Suzuki-Miyaura cross-coupling reaction with aromatic esters and alkyl organoboron reagents as coupling partners. This approach provided a facile route for  $\text{C}(\text{sp}^2)\text{--C}(\text{sp}^3)$  bond formation in a straightforward fashion by successfully inhibiting the undesired  $\beta$ -hydride elimination process. The switch in selectivity is attributed to the judicious selection of different phosphorus ligands that significantly convert the



**Scheme 8** Ni-catalyzed ligand-controlled cross-dimerization and -trimerization of alkynes [28] (color online).



(b) Proposed mechanism

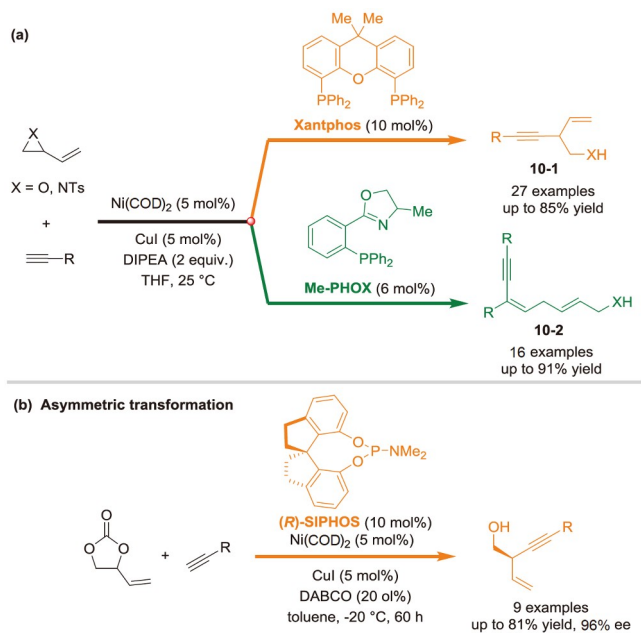


**Scheme 9** Ni-catalyzed switchable bis-thiolation of acetylene with aryl disulfides [29] (color online).

esters into the alkylated and ketone products **11-1** and **11-2**, respectively (Scheme 11a).

DFT studies were carried out in order to rationalize this intriguing reaction chemoselectivity (Scheme 11b). When bidentate phosphorus ligand dcype is used, the nickel complex favors the C(aryl)–C bond cleavage in the oxidation addition step, leading to the alkylated product **11-1** via a decarbonylative process. On the other hand, the nickel complex with monodentate phosphorus ligands, such as  $\text{PBu}_3$  and  $\text{PCy}_3$ , favors activation of the C(acyl)–O bond, which later generates the ketone product **11-2**.

Recently, Jarvo and co-workers [32] revealed ligand-controlled chemoselective switching between one- and two-electron pathways in competing reactions of 4-halotetrahydropyrans. If the reaction is initiated by halogen atom transfer of the alkyl halide, the tetrahydropyran **12-1** will be produced through the alkyl radical intermediate **12-2** (one-

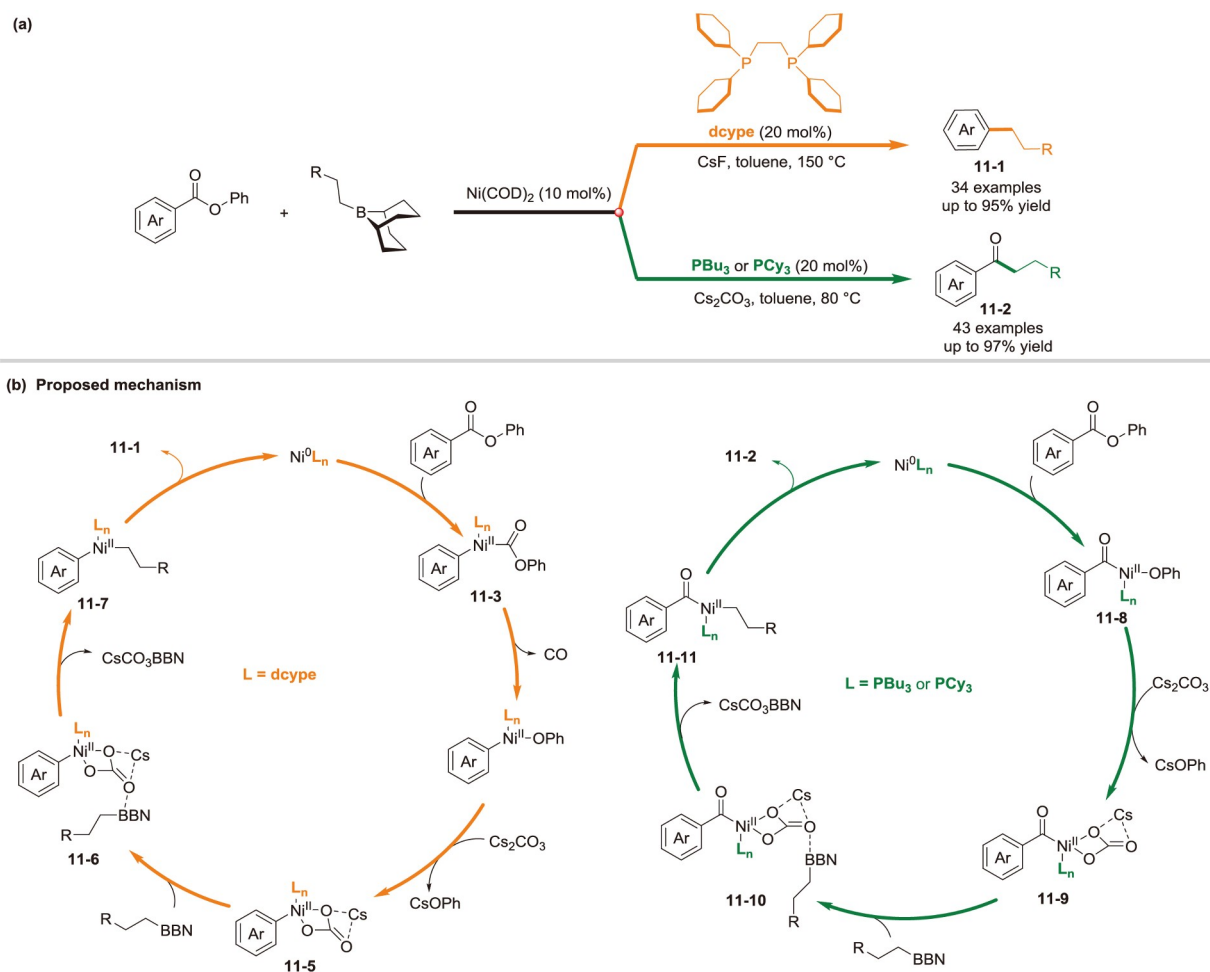


**Scheme 10** Nickel/copper dual-catalyzed divergent allylic alkylation of vinyl epoxides using alkynes [30] (color online).

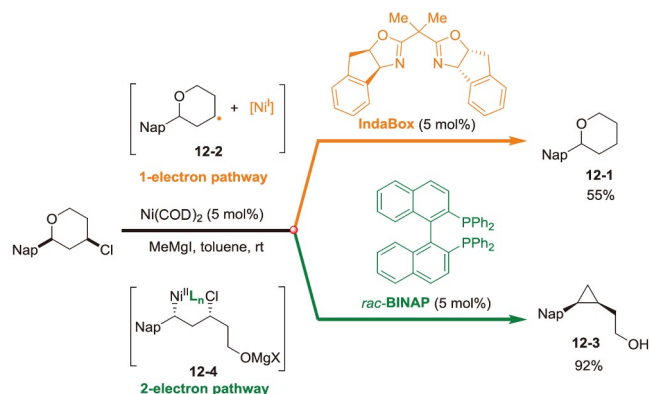
electron pathway). Alternatively, intramolecular cross-electrophile coupling proceeds through the two-electron pathway to afford cyclopropane **12-3**, where oxidative addition occurs *via* an  $S_N2$ -type transition state **12-4** (Scheme 12).

The reason for the chemoselectivity is attributed to the nitrogen-ligated nickel catalyst's preference for a one-electron pathway, initiating halogen atom transfer. In contrast, the phosphine-coordinated nickel catalysts favor closed-shell oxidative addition.

Transition-metal-catalyzed intermolecular [2+2+2] cycloaddition is one of the most powerful methods for the one-step construction of complex bicyclic molecules. However, intermolecular [2+2+2] cycloaddition involving two alkene units has rarely been reported. In 1999, Montgomery and co-workers [33] reported the nickel-catalyzed [2+2+2] cycloaddition of 1,6-enynes with enones. Subsequently, Ogoshi and co-workers [34] disclosed a Ni-catalyzed [2+2+2] cycloaddition of two enones with alkynes. In 2012, Tanaka *et al.* [35] reported the first enantioselective [2+2+2] cycloaddition of ene-allenes and alkenes using cationic rhodium catalysis. Almost simultaneously, Alexanian *et al.* [36]



**Scheme 11** Ni-catalyzed site-selective Suzuki-Miyaura cross-coupling of aromatic esters and alkyl organoborons [31] (color online).



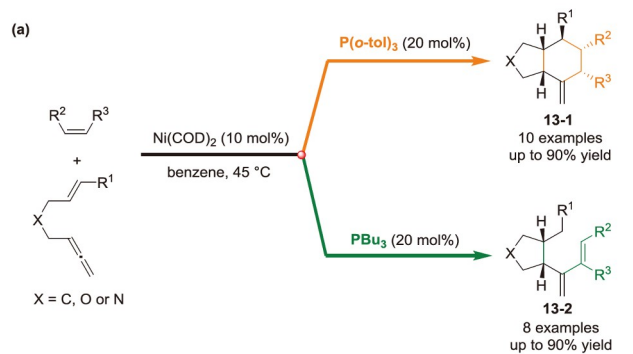
**Scheme 12** Ni-catalyzed switching chemoselectivity from one-electron to two-electron pathways [32] (color online).

developed Ni-catalyzed [2+2+2] cycloadditions and alkenylative cyclizations of ene-allenes and alkenes. When  $P(o\text{-tol})_3$  was used as a ligand, [2+2+2] cycloaddition products **13-1** were obtained exclusively. Interestingly, exchanging  $P(o\text{-tol})_3$  for  $\text{PBu}_3$  led to alkenylative cyclization products **13-2** in high yields with high diastereoselectivity (Scheme 13a).

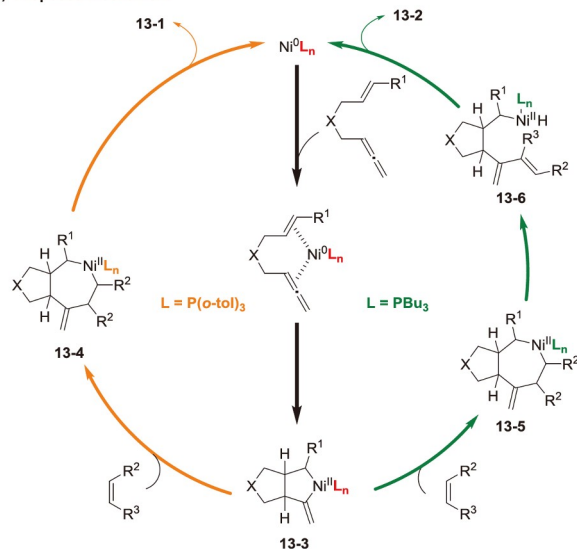
A possible mechanism was depicted in Scheme 13b. Oxidative cyclization of ene-allene provides *cis*-fused bicyclic nickelacycle **13-3**. Using the bulky  $P(o\text{-tol})_3$  as a ligand, direct reductive elimination of **13-4** provides the [2,2,2] cycloadduct **13-1**. The use of less bulky and electron-rich  $\text{PBu}_3$  as a ligand preferentially leads to  $\beta$ -hydride elimination to give nickel hydride **13-6**. Reductive elimination then provides the alkenylative cyclization product **13-2**.

Silacycles are attractive organosilanes because they are widely used in developing  $\pi$ -conjugated organic materials with unique optical and electronic properties. In 1975, Sakurai and Imai [37] reported the first Pd-catalyzed cycloaddition reaction of the silacyclobutane with alkynes, giving the silacyclohexenes **14-1**. Subsequently, Oshima and Utimoto *et al.* [38] investigated the reaction further and found that a large amount of by-product allylsilane **14-2** was formed. Using a sterically demanding chiral phosphoramidite ligand, Shintani and Hayashi *et al.* [39] developed an asymmetric version of this approach for the synthesis of enantiomerically enriched silacyclohexenes **14-1**. An Rh-catalyzed cycloaddition reaction of silacyclobutanes with unactivated alkynes to form silacyclohexenes **14-1** was realized by the Song group [40]. Very recently, Zhao *et al.* [41] reported Ni-catalyzed ligand-controlled cycloaddition or ring-opening coupling of silacyclobutanes and internal alkynes (Scheme 14a).

A plausible mechanism to rationalize the ligand-controlled structure divergence was proposed in Scheme 14b. Two pathways share a Ni-silacycloheptene intermediate. IPr ligand promotes direct reductive elimination *via* a three-membered ring transition state from this intermediate to afford silacyclohexene **14-1**. Alternatively, phosphine ligand



(b) Proposed mechanism



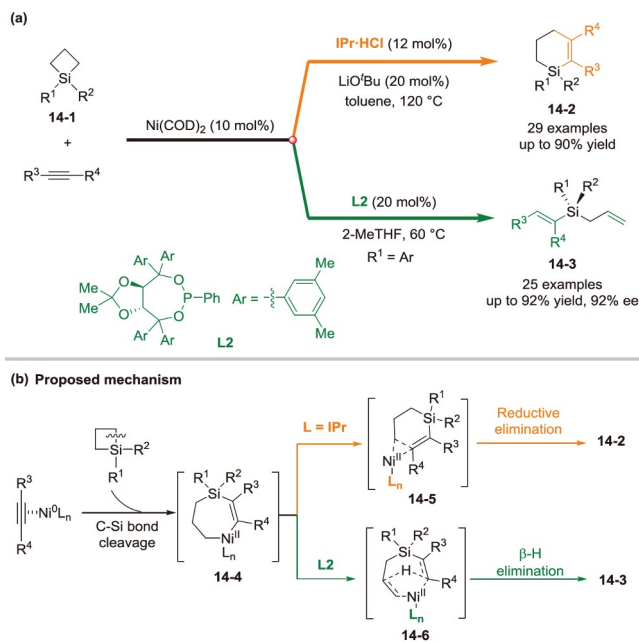
**Scheme 13** Ni-catalyzed [2+2+2] cycloaddition or alkenylative cyclization of ene-allenes and alkenes [36] (color online).

(**L2**) enables ring-opening *via* a ligand-to-ligand H transfer process from Ni-silacycloheptene to generate vinylsilane **14-2**.

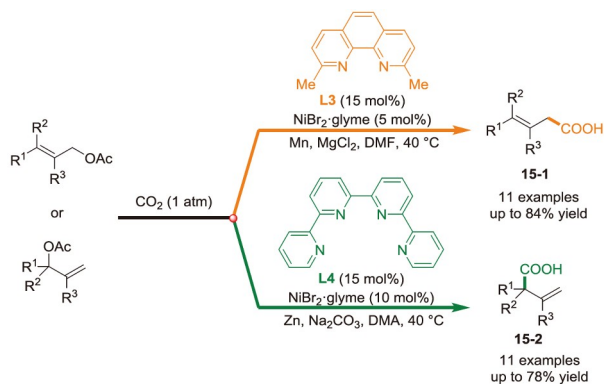
### 3 Regioselectivity

#### 3.1 Regiodivergent functionalization of allylic alcohols

Allyl electrophiles have been successfully employed as coupling partners with nucleophilic counterparts, but controlling the regioselectivity of the allylation reaction remains challenging due to the difficulty in distinguishing the two ends of the initially formed  $\pi$ -allyl metal complex. In 2014, Martin *et al.* [42] reported a Ni-catalyzed ligand-controlled regiodivergent reductive carboxylation of allyl esters with carbon dioxide (Scheme 15). The protocol is modular, allowing for the introduction of the carboxylic motif at any site of the allyl terminus, depending on the ligand used. The C2-methyl substituted bipyridine **L3** ligand was particularly effective for obtaining the linear carboxylic acids **15-1**. In the presence of quaterpyridine **L4**, branched carboxylic acids **15-2** can be generated with high selectivity. The ligand backbone dictates the selectivity pattern and strongly



**Scheme 14** Ni-catalyzed regiodivergent cycloaddition or ring-opening coupling of silacyclobutanes and internal alkynes [41] (color online).



**Scheme 15** Ni-catalyzed regiodivergent carboxylation of allyl esters with carbon dioxide [42] (color online).

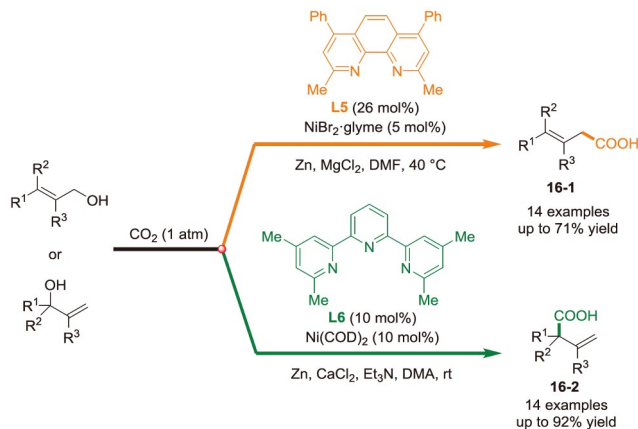
suggests that **L4** may behave similarly to pincer-type ligands through the  $\eta^1$ -allyl intermediate, while the additional pyridine motif may act as a hemilabile ligand.

Unlike the common C–C bond formation with activated organic sulfonates, esters, and ethers, the use of simple alcohols as counterparts, arguably the most accessible and simplest C–O derivatives, has received much less attention due to the significant activation barrier required for C–OH cleavage as well as high polarizability of the O–H bond. The same group further described a Ni-catalyzed switchable site-selective carboxylation of allylic alcohols with CO<sub>2</sub> (Scheme 16) [43]. In the presence of the phenanthroline ligand **L5**, linear carboxylic acids **16-1** were obtained with high regioselectivity. In contrast, the use of bathocurprone (**L6**) as a ligand led to the formation of branched carboxylic acids **16-**

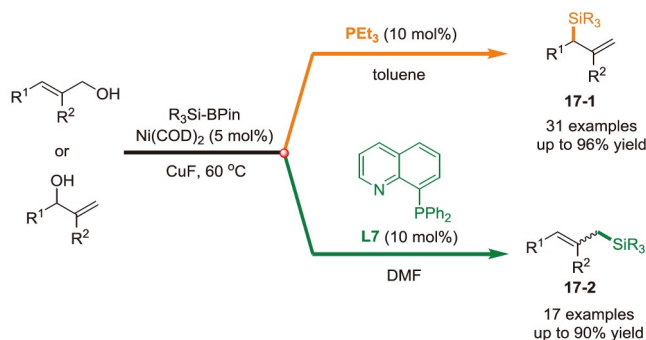
**2**. CO<sub>2</sub> reversibly reacts with alcohols en route to carbonic acids, thereby reducing the activation energy to promote C–O scission while accelerating the rate of oxidative addition to Ni(0) species to allyl alcohol.

In 2019, Liu *et al.* [44] reported a Ni/Cu-catalyzed reiodivergent synthesis of linear and branched allylsilanes directly from allylic alcohols through modulating the steric and electronic properties of the ligands on the nickel catalyst (Scheme 17). When less-hindered ligand PEt<sub>3</sub> was used, branched allylsilanes **17-1** were generated with high selectivity. On the other hand, the use of a bulky ligand 8-(diphenylphosphine)quinoline (**L7**) led to the linear allylsilanes **17-2** formation with high selectivity. Mechanistic studies found that Si–B reagent can be directly activated by CuF<sub>2</sub>. Allyl–OBpin is the key intermediate of the reaction, which may serve as an activated intermediate for the oxidative addition of C(allyl)–O bond.

In 2021, Fang and co-workers [45] reported a Ni-catalyzed regiodivergent cyanation of allylic alcohols, providing an efficient method to access both linear and branched alkenyl nitriles. Moreover, dinitriles can also be obtained in good yields with high selectivity from the corresponding allylic alcohols by a further hydrocyanation process (Scheme 18).

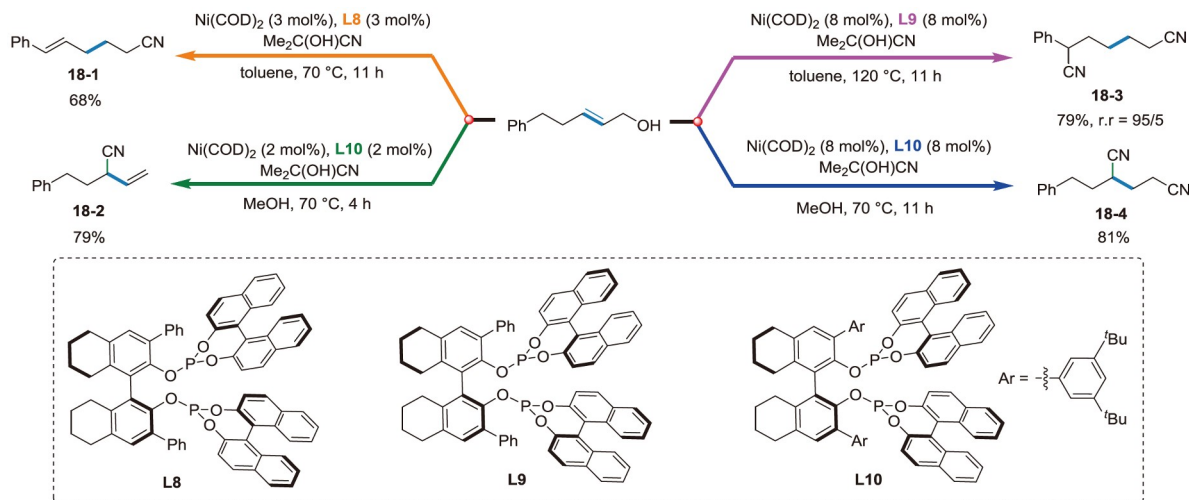


**Scheme 16** Ni-catalyzed site-selective carboxylation of allylic alcohols with carbon dioxide [43] (color online).



**Scheme 17** Ni/Cu-catalyzed ligand-controlled regiodivergent silylation of allylic alcohols [44] (color online).





**Scheme 18** Ni-catalyzed regiodivergent cyanation of allylic alcohols [45] (color online).

Previous studies have shown that the reductive elimination of the  $\pi$ -allyl Ni(II) intermediate determines the regioselectivity. DFT calculations showed that the diastereoisomers **L8** and **L9** construct significantly different pockets around the Ni atom that lead to different environments for the reductive elimination process. **18-3** is formed in the linear selective cyanation step followed by chain-walking along the alkene. **18-4** is conversely formed through a branch-selective transformation. The subsequent hydrocyanation step is probably the rate-determining step.

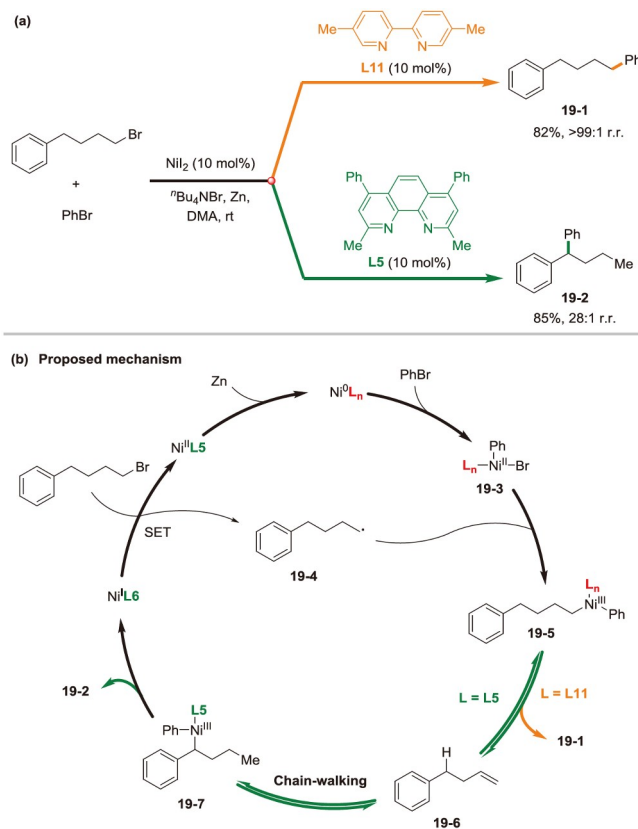
### 3.2 Regiodivergent functionalization of alkyl halides

Alkyl electrophiles are ideal precursors for the construction of  $C(sp^3)-C$  bonds due to their abundance and cheapness. However, the use of alkyl electrophiles in cross-coupling reactions has traditionally been limited by slow oxidative addition or transmetalation, as well as decomposition by fast  $\beta$ -hydride elimination. Although nickel-catalyzed reductive cross-coupling reactions have emerged as a promising method for coupling  $C(sp^3)$  electrophiles, the regioselectivity of these transformations has rarely been explored, with mainly the formation of *ipso*-selective products reported.

In 2018, Yin *et al.* [46] demonstrated a nickel-catalyzed regiodivergent reductive cross-coupling of alkyl bromides with aryl bromides (Scheme 19a). Employment of 5,5'-dimethylbipyridine (**L11**) as the ligand gave the *ipso*-site cross-coupling products **19-1** in 82% yield with exclusive regioselectivity. The reaction with 2,9-dimethyl substituted 1,10-phenanthroline (**L5**) selectively yielded the benzylic phenylation product **19-2**.

A possible mechanism was proposed in Scheme 19b. Selective oxidative addition of Ni(0) to phenyl bromide affords a phenyl-Ni(II) intermediate **19-3**, which reacts with an alkyl radical **19-4** generated *via* single-electron transfer process to

afford Ni(III) intermediate **19-5**. Direct reductive elimination of intermediate **19-5** will yield the *ipso*-coupling product **19-1**. Alternatively, multiple rapid and reversible  $\beta$ -hydride elimination and reinsertion of the resulting double bond leads to the formation of the thermodynamically stable benzylic-Ni(III) intermediate **19-7**. Reductive elimination then yields the 1,1-diarylalkane **19-2**.

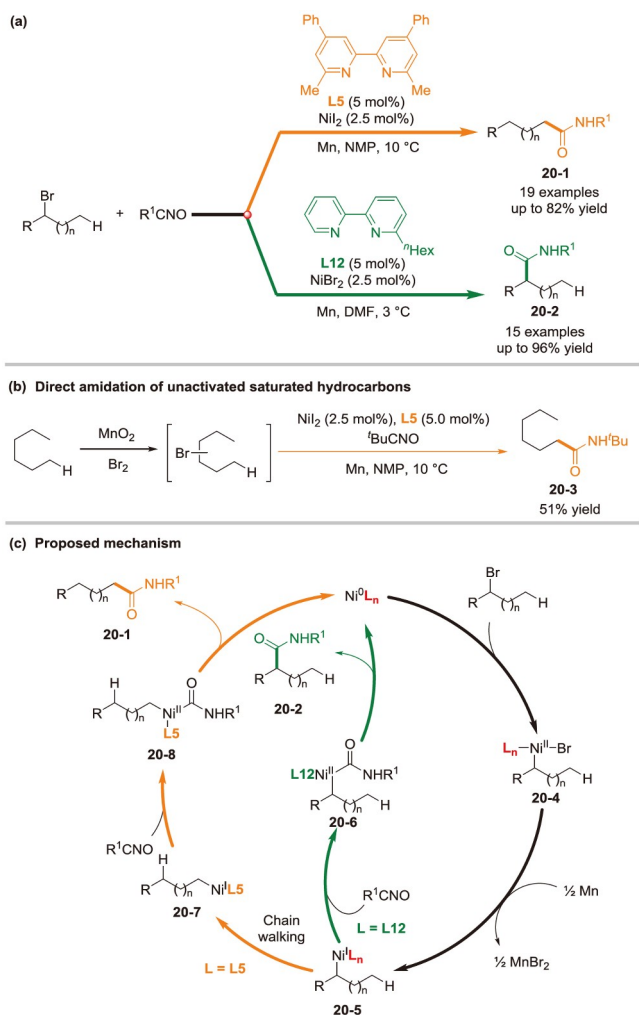


**Scheme 19** Ni-catalyzed regiodivergent reductive cross-coupling of 1-bromo-3-phenylpropane and bromobenzene [46] (color online).

Martin *et al.* [47] disclosed a nickel-catalyzed regiodivergent amidation of secondary alkyl bromides with isocyanate (Scheme 20a). The site selectivity of the amidation event is determined by a subtle modification of the ligand backbone, allowing the introduction of the amide function at either the original  $sp^3$  carbon-halide bond (20-2) or at distal  $sp^3$  C–H sites (20-1) within an alkyl side-chain *via* chain-walking scenarios. The synthetic applicability of the method was demonstrated in Scheme 20b. 20-3 was exclusively obtained from *n*-hexanes *via* a sequence consisting of an unselective  $sp^3$  bromination followed by an amidation at the primary  $sp^3$  C–H bond.

The regioselectivity is attributed to a more congested environment in alkyl-Ni(II)(L)Br 20-5, thus facilitating halide dissociation en route to cationic intermediates that might favor a chain-walking scenario *via* iterative sequences of  $\beta$ -hydride elimination/migratory insertion events (Scheme 20c).

Very recently, Shu *et al.* [48] reported a Ni-catalyzed ligand-controlled regiodivergent cross-electrophile coupling



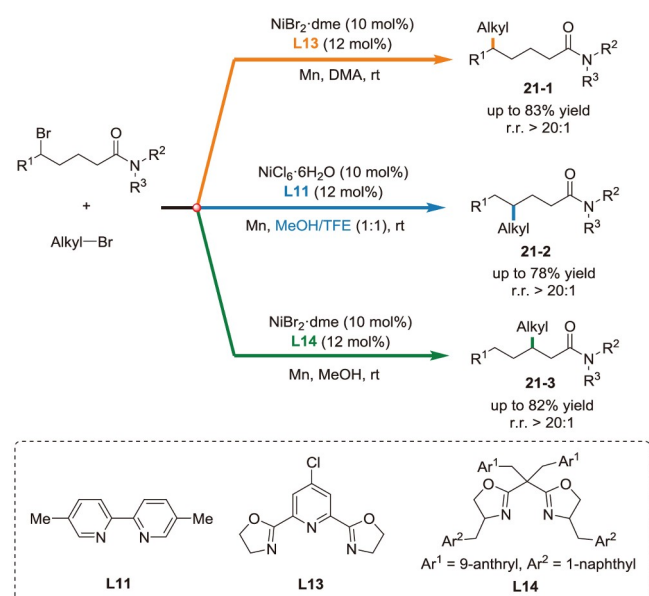
**Scheme 20** Ni-catalyzed regiodivergent amidation of secondary alkyl bromides and isocyanate [47] (color online).

of two distinct alkyl bromides, providing access to  $\beta$ -,  $\gamma$ -,  $\delta$ -alkylated amides (Scheme 21). Using a tridentate ligand (L13), cross-couplings occurred selectively at *ipso*-carbon to form the  $\delta$ -alkylated products 21-1. The  $\gamma$ -alkylation products 21-2 were obtained with high regioselectivity in the presence of 5,5'-dimethyl-2,2'-bipyridine (L11) as a ligand. In addition, the  $\beta$ -alkyl-alkyl coupling product 21-3 could also be obtained by using the bulky BOX ligand L14 and MeOH as solvent. It is worth mentioning that although the authors propose that the selectivity of the product is regulated by the ligands, the solvent also plays a very important role.

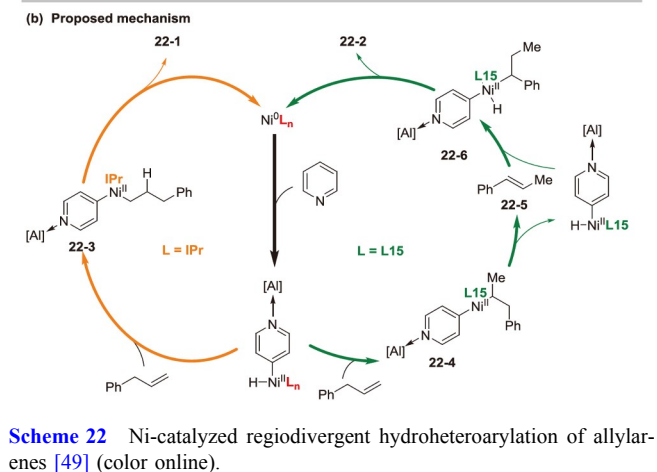
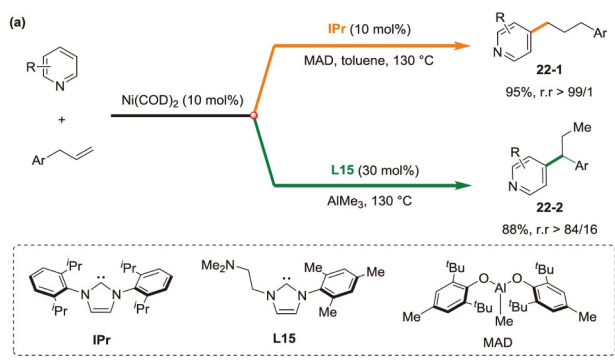
### 3.3 Regiodivergent functionalization of alkenes

Transition-metal-catalyzed hydroarylation of alkenes has attracted extensive attention as one of the most atom-economical and versatile protocols for the construction of functionalized aromatic rings. The hydroarylation of vinylarenes can offer either 1,1-(branched)- or 1,2-(linear)-diarylethyl structural motifs, which are found in many medicinally active molecules and natural products. In 2015, Ong's group [49] disclosed a nickel-catalyzed *para*-CH activation of pyridines with switchable regioselective hydro-heteroarylation of allylarenes. Linear hydrogenated heteroarylation product 22-1 can be selectively generated through the combination of the bulky NHC ligand (IPr) and Lewis acid (MAD). Branched product 22-2 was achieved with moderate selectivity by using a combination of sterically less hindered amino-NHC ligand (L15) and AlMe<sub>3</sub> (Scheme 22a).

A possible mechanism was proposed in Scheme 22b. The



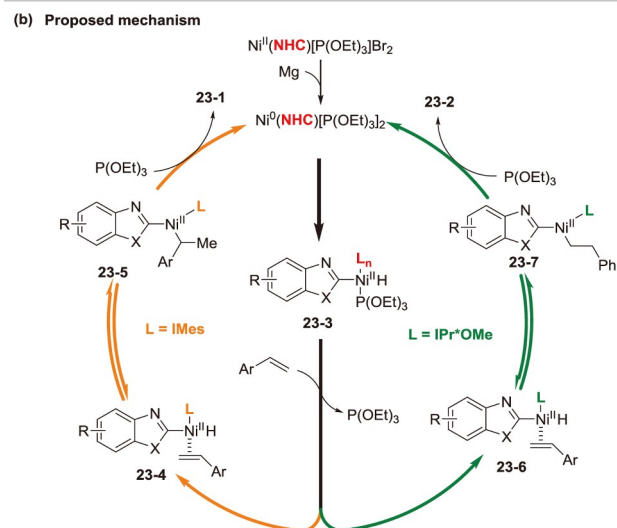
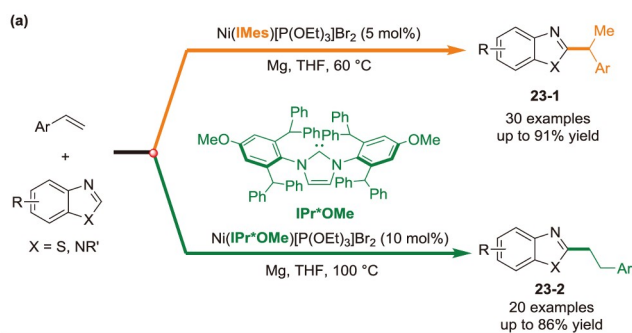
**Scheme 21** Ni-catalyzed regiodivergent cross-electrophile alkyl-alkyl couplings [48] (color online).



formation of linear product **22-1** may be attributed to bulky ligand and bulky Lewis acid-promoted anti-Markovnikov hydronickelation of alkene. In the presence of a sterically less hindered amino-NHC ligand (**L15**), isomerization of the terminal allylarene *via* formal 1,3-hydride shift through migratory insertion of alkene into Ni-H followed by  $\beta$ -H elimination affords the more thermodynamically stable internal styrene **22-5**. Further migratory insertion of **22-5** into Ni-H species gives **22-6**, followed by reductive elimination to form branched product **22-2**. This process may be due to the facile isomerization of olefins and the slow activation of C-H bonds. The rate-determining step is most likely the  $\pi$ -coordination of pyridine onto the metal prior to the C-H bond cleavage or the reductive elimination step.

Nickel sources for the Ni-catalyzed hydroarylation of vinylarenes with heteroarenes have been limited to the use of Ni(COD)<sub>2</sub>, but zerovalent nickel source has inherent drawbacks, including being highly air sensitive, difficult to be handled, and expensive. In 2019, Sun *et al.* [50] synthesized a new class of heteroleptic Ni(II) complexes (Ni(NHC)-[P(OR)<sub>3</sub>]<sub>2</sub>Br<sub>2</sub>) and reported their application in the regiodivergent hydroarylation of vinylarenes with benzothiazoles. Using magnesium turnings as reducing agent, Ni(IMes)[P(OEt)<sub>3</sub>]<sub>2</sub>Br<sub>2</sub> afforded branched products **23-1**, while Ni(IPr\*OMe)[P(OEt)<sub>3</sub>]<sub>2</sub>Br<sub>2</sub> gave linear products **23-2** (Scheme 23a).

A possible mechanism was proposed in Scheme 23b.



Oxidative addition of C<sub>Ar</sub>-H bond to the catalytically active Ni(0) gives heteroleptic nickel hydride **23-3**. Reversible coordination and subsequent insertion into a Ni-H bond followed by reductive elimination afford branched or linear product. Similar to previous reports, the presence of a very bulky IPr\*OMe ligand at the nickel center leads to sterically induced linear selectivity, whereas branched selectivity is due to electronic preference for benzylnickel species.

To date, two strategies have been developed to achieve the hydroarylation of alkenes, which are characterized by different ways to generate the active catalyst species M-H. One uses C-H bond activation of arenes to form M-H, and the other uses hydride reagents to form M-H. However, the former strategy usually requires arenes with a directing group or heteroarenes, while the latter strategy is only effective under reducing conditions. The Zhou group [51] pioneered the study of Ni-catalyzed hydroarylation of alkenes with organoboron compounds under redox-neutral conditions. This transformation was limited to conjugated alkenes, such as styrenes and 1,3-dienes, where the regioselectivity depends on the stability of the corresponding  $\pi$ -benzyl/allyl intermediate. Subsequently, Liu and Engle *et al.* [52] reported a nickel-catalyzed ligand-directed hydroarylation and hydroalkenylation of alkenyl carboxylic acids.

Markovnikov hydrofunctionalization products **24-1** were obtained under ligand-free conditions with selectivities greater than 20:1. Alternatively, anti-Markovnikov products **24-2** were obtained by using a novel 4,4-disubstituted Pyrox ligand (**L16**) with greater than 20:1 selectivity (Scheme 24a).

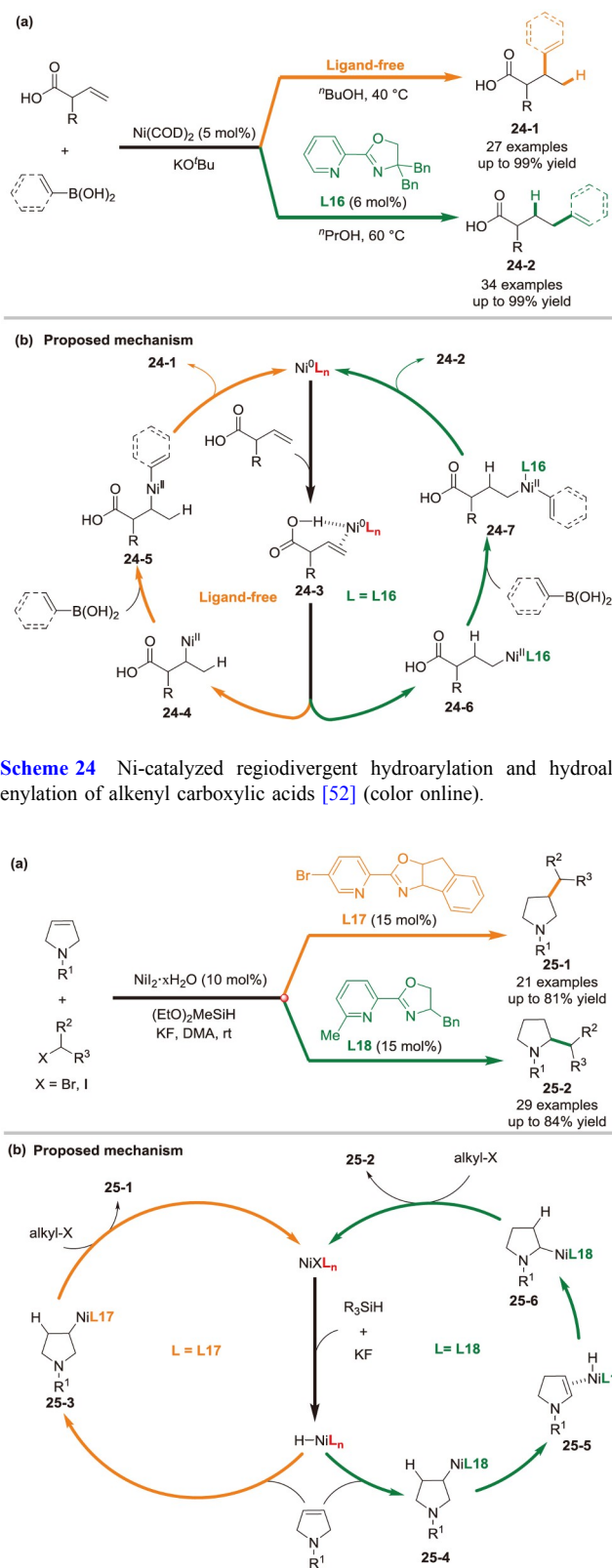
Mechanistic studies revealed that the use of the 4,4-dibenzyl Pyrox ligand (**L16**) leads to a switch in the turnover-limiting step and results in the reversal of regioselectivity compared with ligand-free conditions. DFT calculations indicated that the anti-Markovnikov selectivity is controlled by the steric repulsion between the substrate and the sterically encumbered Pyrox ligand in the transmetalation step (Scheme 24b).

Pyrrolidines with an alkyl substituent at either the 2- or 3-position are present as subunits in many natural products and bioactive molecules. Traditional cross-coupling methods can only perform alkylation at specific and prefunctionalized sites. Hu and co-workers [53] described a ligand-controlled regioselective hydroalkylation of 3-pyrrolines to 2- and 3-alkylated pyrrolidines in good yields. This approach demonstrates broad substrate scope and high functional-group tolerance, and can be utilized in late-stage functionalizations. Pyridine oxazoline ligand (**L17**) favored the C3-alkylated products **25-1**. When the hydrogen at the C6 position of the pyridine oxazoline ligand (**L18**) was replaced by a methyl group, the regioselectivity changed, favoring the generation of C2-alkylated products **25-2** (Scheme 25a).

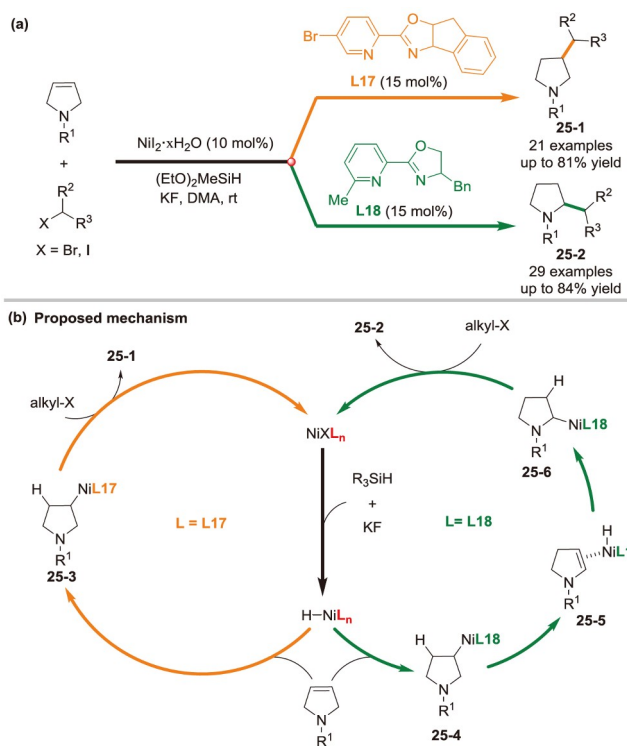
A proposed mechanism was outlined in Scheme 25b. The reaction of nickel precatalyst with silane and in the presence of KF affords Ni-H species, which undergoes migratory insertion to pyrroline to afford the alkyl-Ni intermediate. The direct cross-coupling of intermediate **25-3** with alkyl halides gives C3-alkylation product **25-1**. Intermediate **25-4** can undergo the first  $\beta$ -hydride elimination and then alkene reinsertion to give a second alkyl-Ni intermediate **25-5**, where the Ni fragment is at the position  $\alpha$  to the NR group. Cross-coupling of intermediate **25-6** with alkyl halides gives C2-alkylation product **25-2**. The regioselectivity is attributed to the following two aspects: one is that sterically bulky ligand (**L18**) may favor  $\beta$ -H elimination and subsequent isomerization, and the other is the relative stability of intermediates **25-4** and **25-6**. The nitrogen group in **25-6** is expected to stabilize the nickel center so that C2-alkylation is predominant.

Recently, Zhu and co-workers [54] reported a nickel-catalyzed regioselective reductive hydroarylation of styrenes with aryl triflates. With a diamine ligand (**L19**), the reaction produced the selective linear hydroarylation products **26-1**. Alternatively, with a chiral PyrOx ligand (**L20**), branched 1,1-diaryllalkane products **26-2** were obtained with high regio- and enantioselectivity (Scheme 26).

Wang et al. [55] reported a Ni-catalyzed ligand-controlled, directing group-assisted regioselective migratory hydroalk-

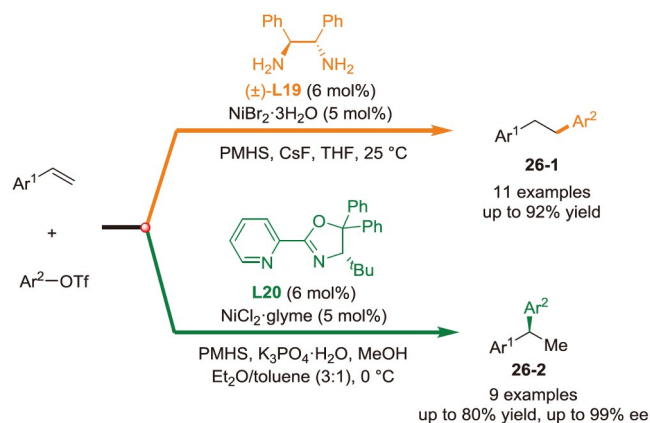


**Scheme 24** Ni-catalyzed regioselective hydroarylation and hydroalkenylation of alkenyl carboxylic acids [52] (color online).



**Scheme 25** Ni-catalyzed regioselective hydroalkylation of 3-pyrrolines and alkyl halides [53] (color online).

ylation of alkenyl amines. A wide range of simple and versatile amides can be used as directing groups, affording  $\alpha$ -



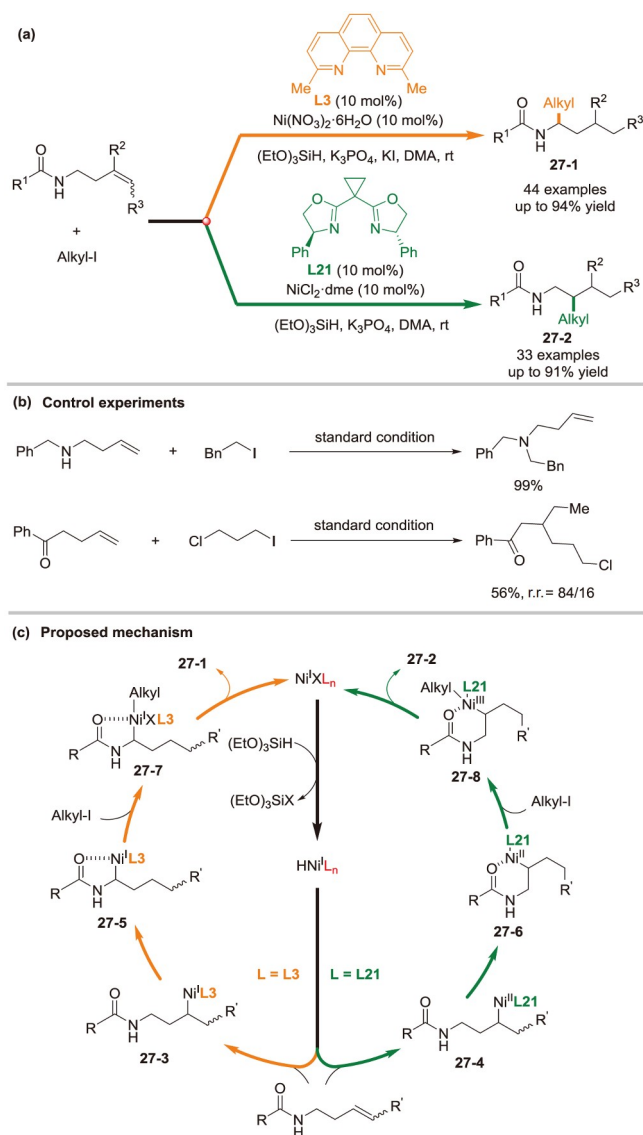
**Scheme 26** Ni-catalyzed regiodivergent hydroarylation of styrenes with aryl triflates [54] (color online).

and  $\beta$ -branched alkyl amines (Scheme 27a). Excellent selectivity to the  $\alpha$ -branched products **27-1** was achieved when **L3** was used as the ligand. Alternatively, the  $\beta$ -branched products **27-2** were obtained with high selectivity when the bisoxazoline ligand **L21** was used.

Control experiments showed that benzyl-protected homoallylamines without a carbonyl group failed to yield the desired product, suggesting that free amine-directing groups are ineffective for hydroalkylation. Hydroalkylation of  $\gamma,\delta$ -alkenyl ketone provided  $\beta$ -selective hydroalkylation products, thus supporting the carbonyl coordination mode. Alkenes with shorter alkyl chains are more reactive, suggesting that the chain-walking process is not rapid and may be the rate-determining step (Scheme 27b).

A possible mechanism was proposed to explain the selectivity of the reaction. Migratory insertion of nickel (I) hydride species into alkene generates alkyl-nickel intermediates (**27-3** and **27-4**), which then undergoes a chain-walking process to afford more stable five- or six-membered nickelacycles (**27-5** and **27-6**). Single-electron transfer of the nickelacycle intermediates with alkyl iodide affords Ni(III) intermediates (**27-7** and **27-8**), followed by reductive elimination to deliver  $\alpha$ - or  $\beta$ -hydroalkylation products **27-1** and **27-2**, respectively (Scheme 27c).

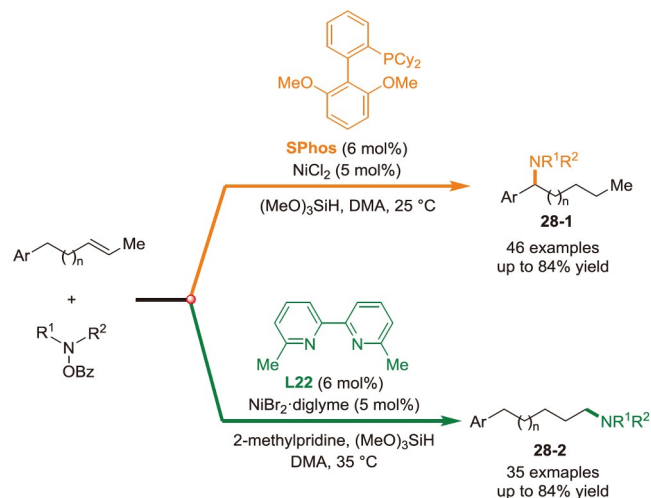
Given the ubiquity of amines in pharmaceuticals, natural products, and agrochemicals, C–N bond formation is crucial in organic synthesis. Hydroamination of alkenes has been recognized as an attractive approach to accessing amines. However, this elegant approach is usually limited to the installation of amino groups on C=C double bonds. Remote functionalization of alkenes remains a formidable challenge in organic synthesis. In 2018, Zhu's group [56] developed a reductive remote hydroamination process *via* a sequential NiH-catalyzed chain walking-reductive hydroarylation relay process. Excellent regio- and chemoselectivity are observed for a wide range of both alkene and nitroarene coupling partners.



**Scheme 27** Ni-catalyzed regiodivergent hydroalkylation of alkenyl amines with alkyl iodides [55] (color online).

Subsequently, Zhu's group [57] demonstrated Ni-catalyzed ligand-controlled regiodivergent hydroamination of alkenes starting from an arbitrary isomer (or isomeric mixtures) of the olefinic substrate, delivering terminal and benzylic C–H amination products with high regioselectivity (Scheme 28). With a rigid and bulky biarylphosphine ligand (SPhos), the reaction led to the selective benzylic C–H amination products **28-1**. Alternatively, the terminal C–H amination products **28-2** were obtained with high regioselectivities using a C2-substituted bipyridine ligand (**L22**).

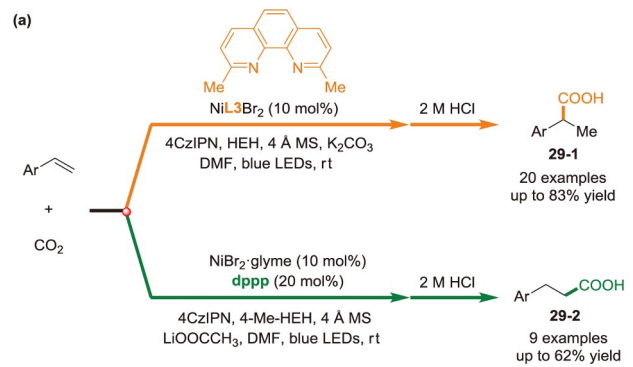
Carboxylation with CO<sub>2</sub> provides direct access to valuable carboxylic acids, which are typically prepared by multistep formylation/oxidation processes. In 2008, Rovis and co-workers [58] reported the first example of nickel-catalyzed reductive carboxylation of styrenes under an atmosphere of CO<sub>2</sub>, providing access to  $\alpha$ -functionalized acids due to the



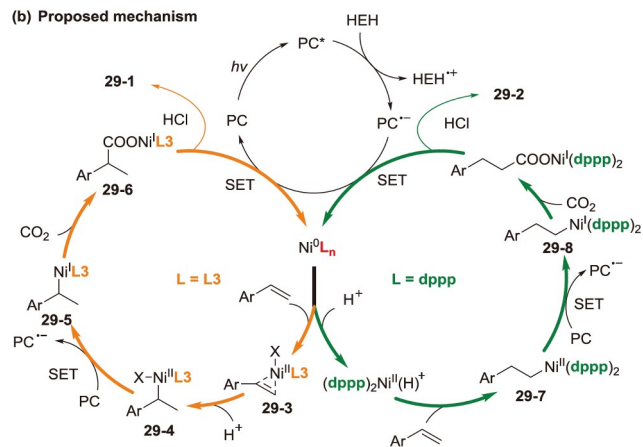
**Scheme 28** Ni-catalyzed regiodivergent hydroamination of alkenes [57] (color online).

formation of the more stable  $\eta^3$ -benzylic metal species. However, the high kinetic and thermodynamic stability of  $\text{CO}_2$  has generally demanded the use of nucleophilic organometallic reagents. Another challenge with direct catalytic hydrocarboxylation using  $\text{CO}_2$  is the limited number of methods to obtain the anti-Markovnikov products. The Jamison's group [59] developed  $\beta$ -selective hydrocarboxylation of styrenes to Markovnikov products under atmospheric pressure of  $\text{CO}_2$  using photoredox catalysis in continuous flow in 2017. König *et al.* [60] further developed ligand-controlled Markovnikov and anti-Markovnikov hydrocarboxylation of styrenes with an atmospheric pressure of  $\text{CO}_2$  at room temperature using dual visible-light-nickel catalysis (Scheme 29a). When neocuproine was used as a ligand (**L3**), the Markovnikov products **29-1** were obtained exclusively. On the other hand, employing dppb as the ligand favored the formation of the anti-Markovnikov products **29-2**. A range of functional groups and electron-poor, -neutral, as well as electron-rich styrene derivatives are tolerated by the reaction, providing the desired products in moderate to good yields. Mechanistic investigations indicate that a nickel (I) hydride species is generated and adds irreversibly to styrenes.

Li *et al.* [61] further performed DFT calculations to understand the reaction mechanism (Scheme 29b). When Ni(II) catalysts with ligands of different properties are used, the Ni centers of the active catalytic species have different valence states. For the neocuproine ligand (**L3**), styrene ligating to the Ni(I) species initiates the hydrocarboxylation, and subsequent protonation occurs preferentially on the  $\beta$ -C atom, which facilitates the following insertion of  $\text{CO}_2$  at the  $\alpha$ -C position and produces unique  $\alpha$ -selective product **29-1**. However, in the presence of dppb as a ligand, the key Ni-hydride intermediate is first formed by the protonation of Ni(0) species. The excellent  $\beta$ -selectivity is attributed to the



**(b) Proposed mechanism**



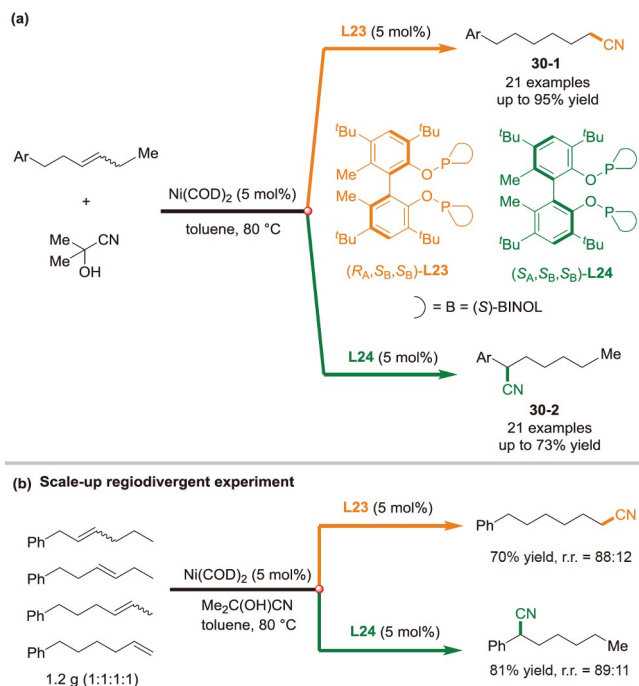
**Scheme 29** Ligand-controlled regioselective hydrocarboxylation of styrenes with  $\text{CO}_2$  via dual visible-light-nickel catalysis [60,61] (color online).

predominance of  $\beta$ -C ligating to the Ni center rather than its protonation.

In 2021, Fang *et al.* [62] reported nickel-catalyzed regiodivergent hydrocyanation of a wide range of internal alkenes via a chain-walking process. When appropriate diastereomeric biaryl diphosphate ligands were applied, the same starting materials can be converted to linear or branched nitriles in good yields with high regioselectivities (Scheme 30a). The utility of this approach was demonstrated by the conversion of unrefined olefin isomers to branched and linear hydrocyanation products at the gram-scale scale (Scheme 30b). DFT calculations revealed that the coordination of diastereomeric bisaryl bisphosphate ligands to Ni led to different catalyst structures, resulting in different regioselectivities through modulation of electronic and steric interactions.

### 3.4 Regiodivergent functionalization of alkynes

Ni-catalyzed reductive coupling of alkynes and aldehydes is an efficient method for the synthesis of allylic alcohols. Alkynes with strong electronic or steric biases often show excellent regiocontrol, but only a single regiochemical outcome is typically available. However, alkynes lacking strong electrons or steric biases generally lead to poor regioselectivity.



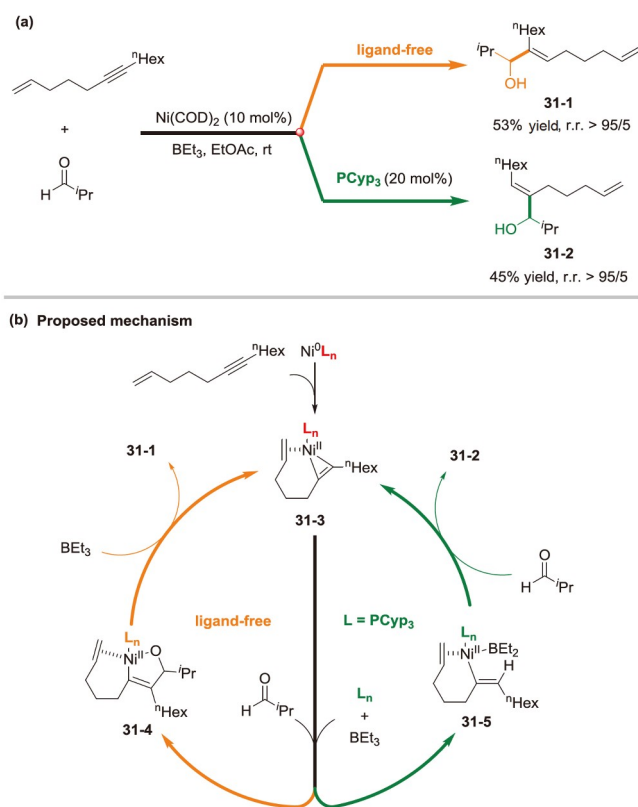
**Scheme 30** Ni-catalyzed regiodivergent hydrocyanation of internal alkenes [62] (color online).

tivity. Controlling the regioselectivity of reductive coupling reaction is extremely challenging. As early as 2003, Jamison *et al.* [63] observed ligand-switchable directing effects of tethered alkenes in nickel-catalyzed additions to alkynes (Scheme 31a). The regioselectivity was determined by distant non-conjugated alkenes and the regioselectivity can be completely reversed (from > 95:5 to 5:>95) in the presence of phosphine ligand (PCyp<sub>3</sub>).

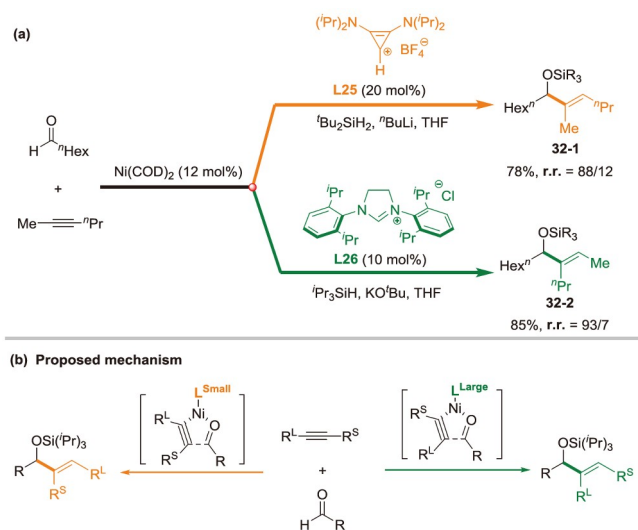
Scheme 31b illustrates the mechanism for the reductive coupling of 1,6-enynes and aldehydes [64]. In the absence of a phosphine ligand, ligand substitution places the aldehyde *cis* to the carbon distal to the alkene, while the alkene is coordinated to the nickel, resulting in the exclusive formation of intermediate **31-4**. PCyp<sub>3</sub> coordinates more strongly to the metal center than the tethered olefin and can thus displace the aldehyde, leading to the formation of regioisomer **31-5**.

Remote directing functionality has proven to be effective in Ni-catalyzed and Ti-promoted reductive coupling of alkynes and aldehydes [65]. Regiochemical control that overrides inherent substrate biases and that does not require the installation of a directing functional group would be the ideal solution [66,67]. In 2010, the Montgomery group [68] reported nickel-catalyzed ligand-controlled aldehyde-alkyne reductive coupling (Scheme 32a). Regioselectivity was primarily controlled by the steric hindrance in the region of the ligand close to the alkyne.

DFT calculation indicated that the control of regioselectivity by ligands is derived from alkyne-ligand interactions



**Scheme 31** Ligand-switchable directing effects of tethered alkenes in Ni-catalyzed reductive coupling of alkynes and aldehydes [63,64] (color online).



**Scheme 32** Ni-catalyzed regiodivergent reductive coupling of aldehydes and alkynes [68,69] (color online).

when large ligands are used, and from aldehyde-alkyne interactions when small ligands are employed, involving the rate-determining oxidative addition (Scheme 32b). The regioselectivities are directly affected by the shape and orientation of the N-substituents on the ligand [69].

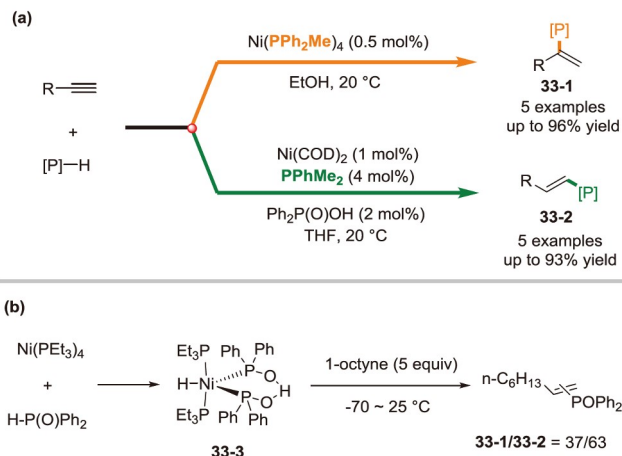
In 2004, Han and co-workers [70] reported a nickel-cata-

lyzed ligand-controlled addition of H-P(O) to alkynes, affording the Markovnikov and anti-Markovnikov adducts **33-1** and **33-2** with excellent selectivity (Scheme 33a). In the presence of the nickel catalyst Ni(PPh<sub>2</sub>Me)<sub>4</sub>, the reaction was carried out in EtOH at room temperature to afford the Markovnikov products **33-1** in good yields with high regioselectivity. Alternatively, when the same reaction was conducted in THF and using PPhMe<sub>2</sub> as a ligand, the selectivity was switched to anti-Markovnikov products **33-2**. Mechanistic studies revealed that the pentacoordinate hydrido nickel complex **33-3** is the key intermediate of the reaction, which is formed through the oxidative addition of Ph<sub>2</sub>P(O)H to NiP(Et<sub>3</sub>)<sub>4</sub> (Scheme 33b). Complex **33-3** may adopt a trigonal bipyramidal structure and favors the formation of anti-Markovnikov products.

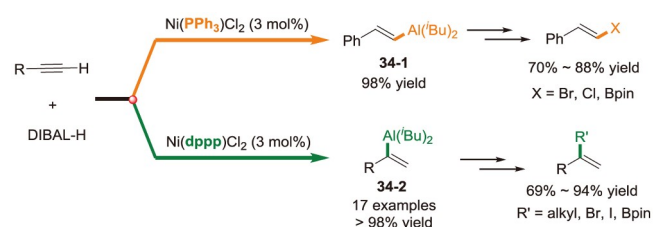
Selective and practical alkyne hydrometalation is of great value, as the resulting vinylmetals can be used to access vinyl halides and borates, which are very important intermediates in cross-coupling reactions. In 2010, the Hoveyda group [71] reported a nickel-catalyzed ligand-controlled regiodivergent hydroalumination of terminal alkynes (Scheme 34). In the presence of a reagent (diisobutylaluminum hydride, DIBAL-H) and Ni(dppp)Cl<sub>2</sub>,  $\alpha$ -vinylaluminum isomers **34-2** were obtained in good yields with high regioselectivity. Under the same conditions, but with Ni(PPh<sub>3</sub>)<sub>2</sub>Cl<sub>2</sub> as the catalyst, hydroalumination switched to highly  $\beta$ -selective. The hydroalumination products could be further converted into the corresponding vinyl halides and boronates with the appropriate electrophiles.

1,3-Enynes are important structural motifs common in many bioactive molecules and organic materials. Hydrofunctionalization of 1,3-diyne paved a new route to access functionalized 1,3-enynes. However, hydrocyanation of 1,3-diyne remained elusive due to the intractable challenges in regio- and stereoselectivity control for unsymmetrical internal alkynes. Fang and co-workers [72] reported a nickel-catalyzed regiodivergent hydrocyanation of 1-aryl-4-silyl-1,3-diyne. When appropriate bisphosphine and phosphine-phosphite ligands were used, the same starting materials were converted into two different enynyl nitriles **35-1** and **35-2** in good yields with high regioselectivities (Scheme 35). DFT calculations showed that the structural features of different ligands lead to different alkyne insertion modes, which in turn lead to different regioselectivities.

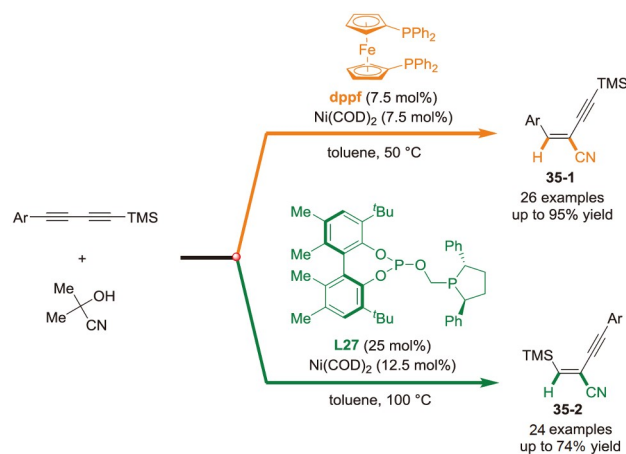
In recent years, metallaphotoredox has emerged as a powerful strategy in which traditionally inert functional groups are readily converted into carbon-centered radicals, which subsequently participate in organometallic cross-couplings *via* a two-stage radical trapping and reductive elimination cycle. Notably, photoredox/nickel dual catalysis has recently found application in the hydroalkylation of terminal and internal alkynes. The Wu group [73] realized the hydroalkylation of internal alkynes with ether and amide



**Scheme 33** Ni-catalyzed regiodivergent addition of H-P(O) to alkynes [70] (color online).



**Scheme 34** Ni-catalyzed regiodivergent hydroalumination of terminal alkynes [71] (color online).



**Scheme 35** Ni-catalyzed regiodivergent hydrocyanation of 1-aryl-4-silyl-1,3-diyne [72] (color online).

C(sp<sup>3</sup>)-H bonds with high selectivity. Decarboxylative hydroalkylation of aliphatic alkynes with alkyl carboxylic acids was also achieved by the MacMillan group [74], giving the corresponding products in Markovnikov regioselectivity. Subsequently, Rueping and co-workers [75] further developed a photoredox/nickel dual-catalyzed anti-Markovnikov-type decarboxylative hydroalkylation of styrenes with alkyl carboxylic acids. Very recently, Nishibayashi *et al.* [76] reported photoredox/nickel dual-catalyzed hydroalkylation of



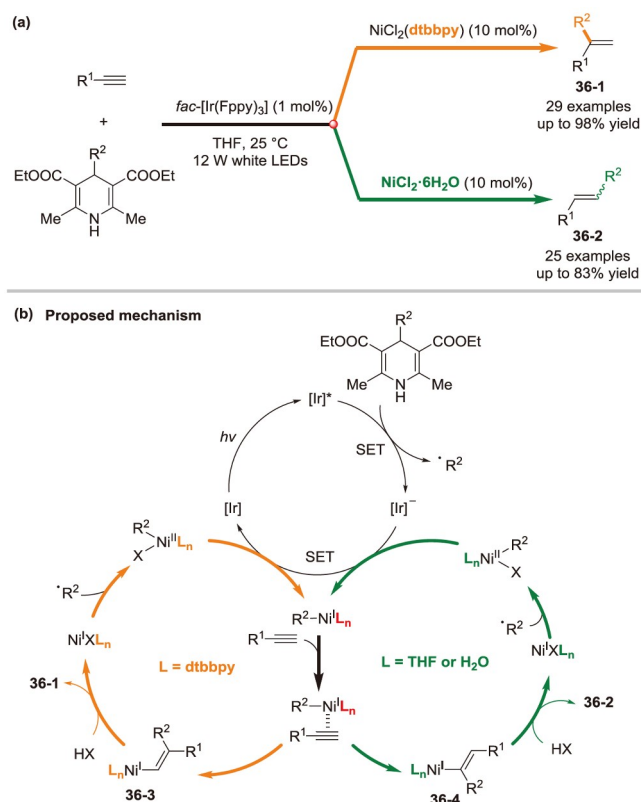
terminal alkynes with 4-alkyl-1,4-dihydropyridines. Using  $[\text{NiCl}_2(\text{dtbbpy})]$  as a catalyst led to the formation of Markovnikov-type products **36-1**, whereas using  $\text{NiCl}_2 \cdot 6\text{H}_2\text{O}$  led to the formation of anti-Markovnikov-type products **36-2** (Scheme 36a).

The proposed mechanism was depicted in Scheme 36b. In the Markovnikov-type pathway, a bulky ligand such as dtbbpy inhibits the formation of anti-Markovnikov-type insertion, leading to the formation of Markovnikov-type intermediate **36-3**. Alternatively, small ligands such as water and THF do not inhibit the anti-Markovnikov-type insertion, leading to the formation of anti-Markovnikov-type intermediate **36-4**.

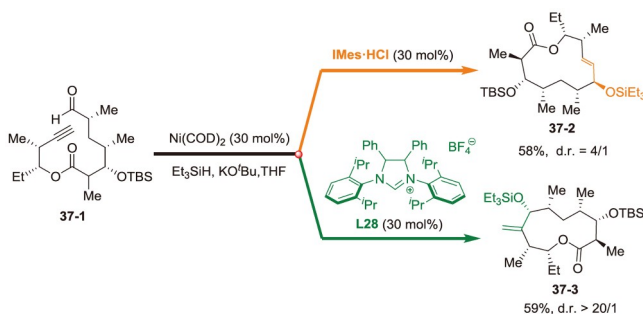
### 3.5 Regiodivergent cyclization

Macrocyclic allylic alcohols are a common structural motif in many natural products. The strategy of preparing macrocyclic allylic alcohols by the nickel-catalyzed reductive *exo*-cyclization of ynals was elegantly applied by Jamison *et al.* [77] in the total syntheses of amphidinolides T1 and T4. A similar approach was explored in the *endo*-cyclization of ynals with internal alkynes in an approach to (–)-terpestacin; however, that strategy was not realized because of the facility of the corresponding *exo*-cyclization [78]. Therefore, it is highly desirable to develop reductive macrocyclization reactions to access both *endo*- and *exo*-manifolds. Montgomery group developed a nickel-catalyzed ligand-controlled regiodivergent reductive macrocyclizations of ynals [79] and applied this method to the synthesis of 10-deoxymethynolide [80]. Selective *endo*-cyclization of the advanced synthetic intermediate **37-1** provided the natural twelve-membered ring **37-2** when IMes was used as a ligand. Alternatively, selective *exo*-cyclization was achieved using the bulky ligand DP-IPr (**L28**) to provide access to the unnatural eleven-membered ring **37-3** (Scheme 37).

The 2-pyridone structural motif is common in natural products and pharmacologically potent compounds displaying a diversity of properties. Nakao, Hiyama, and colleagues [81,82] developed a synergistic nickel(0)/Lewis acid catalyzed intermolecular C6-selective alkylation and alkenylation of pyridones *via* C–H activation/alkene hydroarylation. Intramolecular alkylation of alkene-tethered pyridones afforded mostly the *exo*-cyclization products **38-1** [82]. In principle, both ends of the double bond can be reacted, thus resulting in the formation of either *exo* or *endo*-cyclization products **38-1** and **38-2**. Cramer *et al.* [83] reported a regiodivergent and highly selective synthesis of 1,6-annulated 2-pyridones by intramolecular Ni-catalyzed cyclization (Scheme 38a). The regioselectivity of the cyclization was completely controlled by the ligand and almost independent of the ring size and alkene substitution pattern. In the presence of cyclooctadiene, the *exo*-cyclization products **38-1**



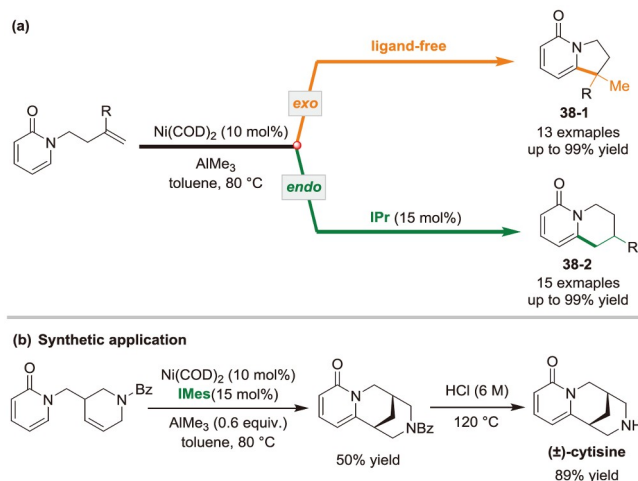
**Scheme 36** Photoredox/nickel dual-catalyzed hydroalkylation of terminal alkynes with 4-alkyl-1,4-dihydropyridines [76] (color online).



**Scheme 37** Ni-catalyzed regiodivergent reductive macrocyclizations of ynals [80] (color online).

were obtained exclusively, whereas the bulky NHC ligand selectively provided the *endo*-cyclized products **38-2**. Moreover, this method was further applied to the synthesis of lupine alkaloid cytisine (Scheme 38b).

Transition-metal-catalyzed alkene dicarbofunctionalization involving intramolecular Heck cyclization and intermolecular cross-coupling is a powerful approach for the construction of cyclic frameworks. However, in the formation of small rings (five-, six-, and seven-membered rings), intramolecular Heck reactions almost always proceed *via* an *exo*-cyclization mode. To date, transition metal-catalyzed difunctionalization of alkenes *via* *endo*-selective cyclization/cross-coupling has not been achieved, which greatly limits

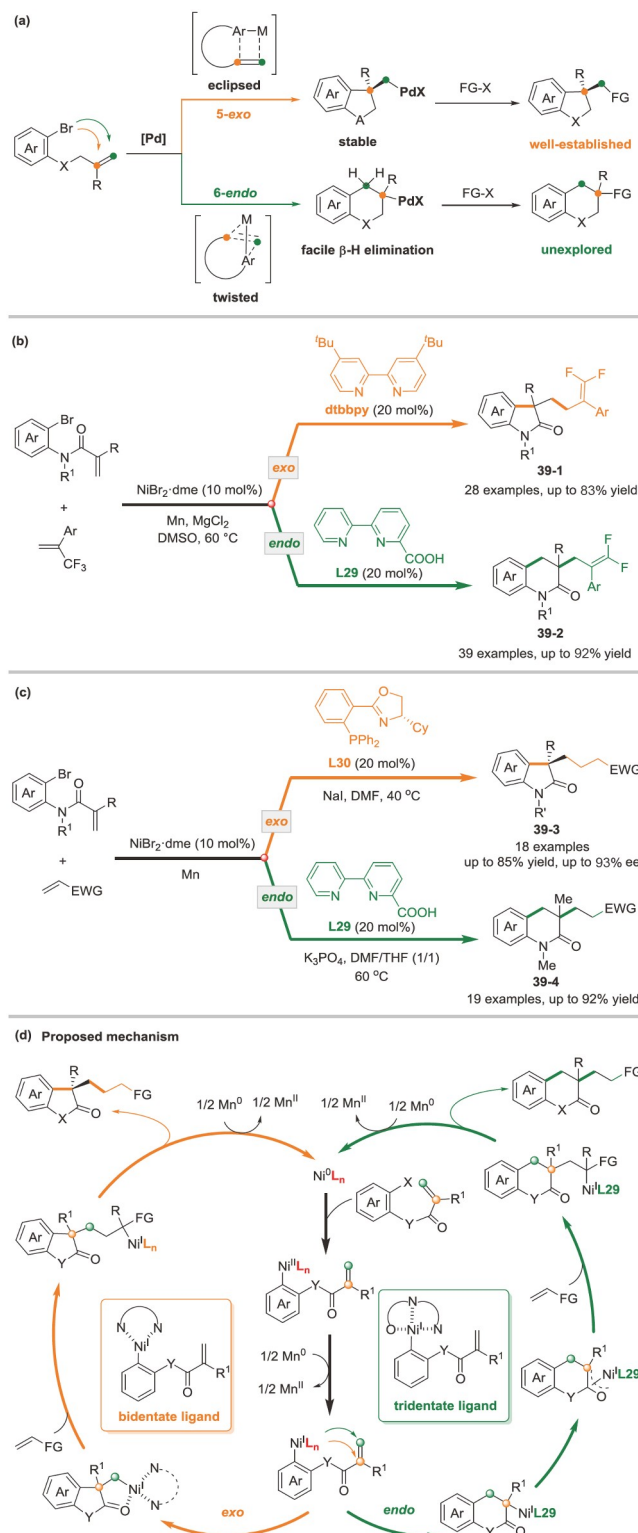


**Scheme 38** Ni-catalyzed regiodivergent *exo*- or *endo*-annulation of pyridines [83] (color online).

the applicability of this method. *Endo*-selective cyclization/cross-coupling is a formidable challenge for the following reasons: (1) Due to the limited tether length, the eclipsed conformations of alkene and Pd-C  $\sigma$ -bond preferentially generate the *exo*-cyclization products, while the *endo*-cyclization requires a longer, more flexible chain to adopt a twisted conformation. (2) *Exo*-cyclized intermediates are relatively stable due to the absence of  $\beta$ -H, whereas *endo*-cyclized intermediates can be rapidly dissociated by  $\beta$ -H elimination. (3) Compared with *exo*-cyclized intermediates, *endo*-cyclized intermediates are difficult to undergo further cross-coupling reactions due to the strong steric hindrance (Scheme 39a).

Kong's group [84] demonstrated the first example of Ni-catalyzed ligand-controlled dicarbofunctionalization of alkenes. Starting from the same substrate, five- or six-membered benzo-fused lactams **39-1** and **39-2** bearing *gem*-difluoromethylene groups can be obtained with excellent regioselectivity, respectively (Scheme 39b). Using a chiral Pyrox- or PHOX-type bidentate ligand, 5-*exo* cyclization/cross-couplings proceed favorably to produce indole-2-ones **39-3** in good yields with excellent regioselectivity and enantioselectivities (up to 98% ee). When C6-carboxylic acid-modified 2,2'-bipyridine was used as the ligand, 3,4-dihydroquinolin-2-ones **39-4** were obtained in good yields through 6-*endo*-selective cyclization/cross-coupling processes (Scheme 39c). This transformation is modular and tolerant for a variety of functional groups.

A plausible mechanism was proposed in Scheme 39d. The carboxylic acid group in **L29** might act as a hemilabile ligand, thus providing flexibility for stabilizing reactive intermediates. It can not only act as a sterically hindered tridentate ligand to regulate *endo*-selective cyclization, but also dissociate into a less sterically hindered bidentate ligand to facilitate the subsequent cross-coupling process.

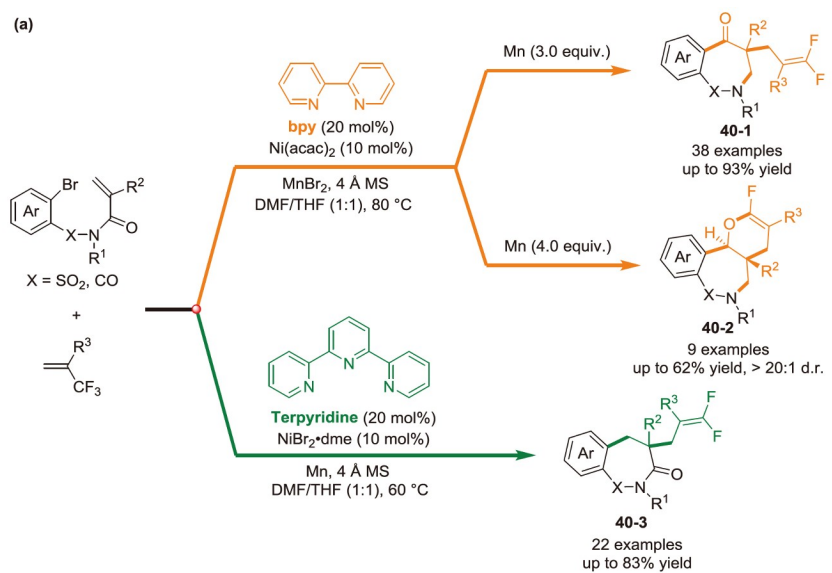


**Scheme 39** Ni-catalyzed regiodivergent reductive dicarbofunctionalization of alkenes [84] (color online).

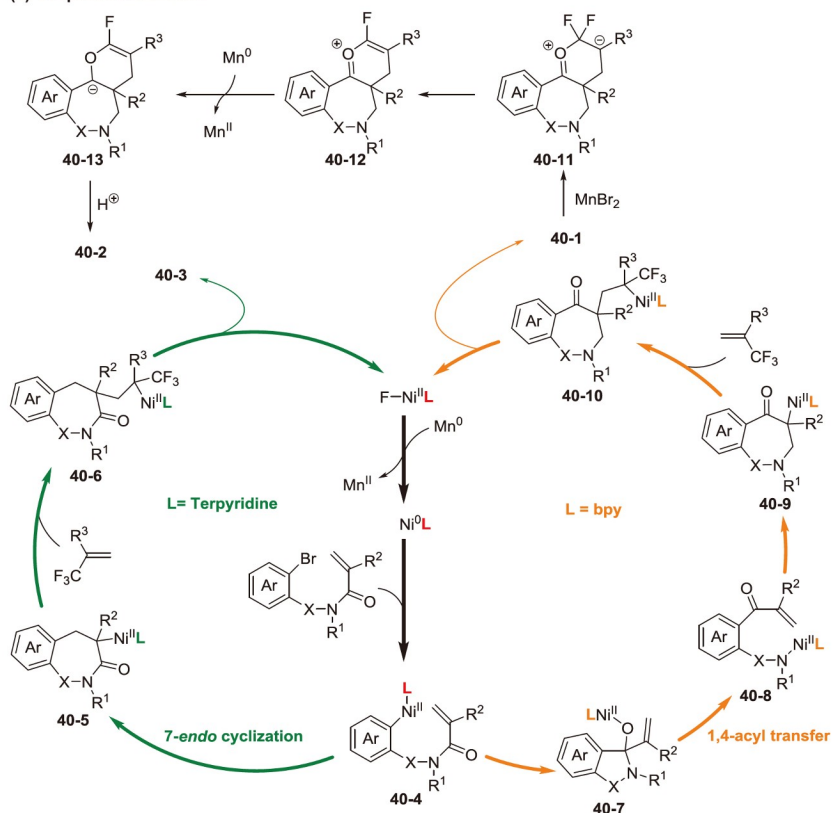
Transition metal-catalyzed intramolecular addition of aryl halides to aldehydes, ketones, and esters has been extensively studied for the construction of benzo-fused heterocycles, but amides have rarely been described. This is

perhaps not surprising since, according to textbook knowledge, the low reactivity of amides stems from amide resonance stability. This resonance stabilization imparts double-bond character to the amide bond while reducing the susceptibility of the amide to nucleophilic attack. Consequently, the direct functionalization of amide bonds under mild and functional-group-tolerant conditions has been a long-standing synthetic challenge. Kong *et al.* [85] designed

acrylamide substrates (*N*-acrylamide and *N*-sulfonylacrylamide) through appropriate steric and electronic activation of the amide N–C(O) bonds, which can extend the cyclization mode to carbonyl groups beyond the C–C double bond. A nickel-catalyzed ligand-controlled cyclization/cross-coupling was thus achieved, enabling the divergent synthesis of pharmacologically important 2-benzazepine frameworks (Scheme 40a).



(b) Proposed mechanism



Scheme 40 Ni-catalyzed divergent synthesis of 2-benzazepine derivatives [85] (color online).

The bidentate ligand (bpy) facilitates the nucleophilic addition of the aryl halides to the amide carbonyl, followed by 1,4-acyl transfer and cross-coupling to obtain 2-benzazepin-5-ones **40-1** and benzo[*c*]pyrano[2,3-*e*]azepines **40-2**. The tridentate ligand (terpyridine) promotes the selective 7-*endo* cyclization/cross-coupling to access 2-benzazepin-3-ones **40-3**.

The possible reaction mechanism was proposed in [Scheme 40b](#). When the tridentate ligand (terpyridine) is used, 7-*endo* cyclization is favored to give the aza-seven-membered-ring nickel(II) intermediate **40-5**. Migratory insertion of Ni(II) species **40-5** to trifluoromethyl alkene followed by  $\beta$ -F elimination provides 2-benzazepin-3-ones **40-3**. In the presence of bidentate ligand (bpy), the ground-state destabilization amide allows the nucleophilic addition of Ar-Ni(II)X intermediate **40-4** to the amide carbonyl group to form the tetrahedral Ni(II) alkoxide intermediate **40-7**, which would undergo ring opening with 1,4-acyl transfer *via* C–N bond cleavage, resulting in the amide-Ni(II) intermediate **40-8**. Intramolecular aza-Michael addition of the amide-Ni(II) intermediate **40-8** will lead to the 7-membered ring Ni(II) intermediate **40-9**, which undergoes similar migratory insertion to trifluoromethyl alkene followed by  $\beta$ -F elimination to provide 2-benzazepin-5-ones **40-1**.

Notably, the MnBr<sub>2</sub> could serve as an electrophilic Lewis acid to activate the *gem*-difluoroalkene moiety, promoting the intramolecular nucleophilic cyclization to give **40-11**. Fluorine elimination followed by Mn<sup>0</sup> reduction yields the cyclic carbanion intermediate **40-13**, which affords benzo[*c*]pyrano[2,3-*e*]azepine **40-2** upon protonolysis.

The same group further reported an unprecedented ligand-switchable nickel-catalyzed dyotropic rearrangement, in which the ligands could control the migratory aptitude of different groups by modifying the ligands on the metal catalyst and changing the oxidation states of the metal, providing the divergent synthesis of four medicinally relevant fluorine-containing scaffolds from the same starting material ([Scheme 41a](#)) [86]. The sterically hindered <sup>i</sup>PrPDI ligand (**L31**) facilitates 1,2-aryl/Ni dyotropic rearrangement, while the terpyridine ligand promotes 1,2-acyl/Ni dyotropic rearrangement.

A plausible mechanism was demonstrated in [Scheme 41b](#). The tridentate chelating ligand facilitates 6-*exo* cyclization to obtain  $\sigma$ -alkyl-Ni(II)X intermediate **41-5**, which could be reduced by Mn to form a more nucleophilic  $\sigma$ -alkyl-Ni(I) species **41-6**. The sterically hindered ligand <sup>i</sup>PrPDI (**L31**) favors the 1,2-aryl/Ni dyotropic rearrangement to form nickel(I) **41-7**, which undergoes migratory insertion into trifluoromethyl alkene followed by  $\beta$ -F elimination furnishing product **41-1**. Alternatively, terpyridine promotes the 1,2-acyl/Ni dyotropic rearrangement to form nickel(I) intermediate **41-9**. Nucleophilic addition to trifluoromethyl alkene forms the carbonickelation adduct **41-10**. Intramolecular nucleophilic addition to the amide's carbonyl fol-

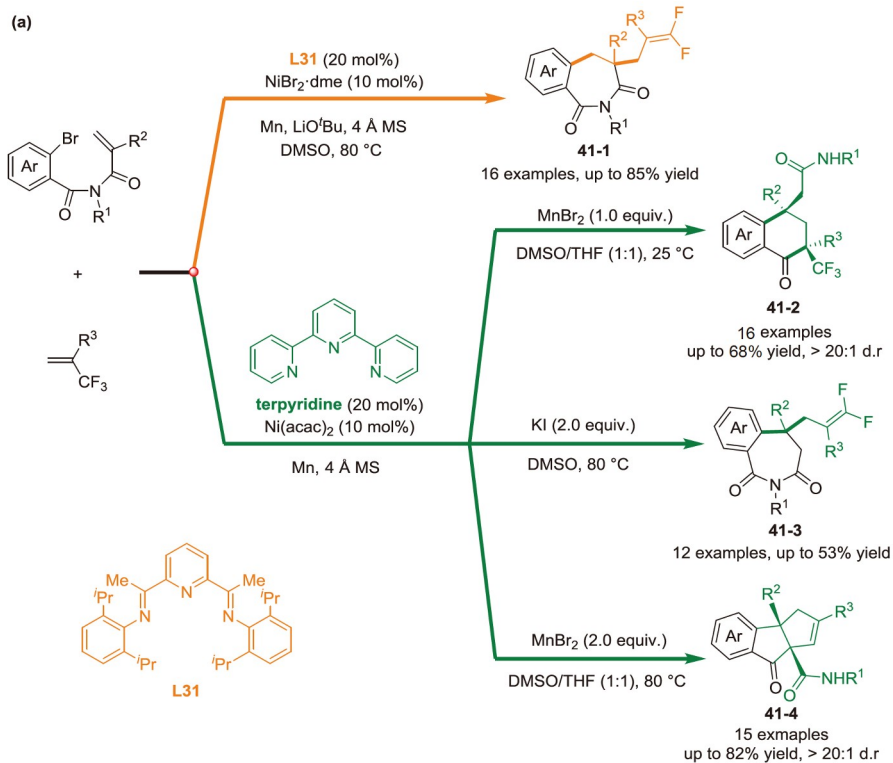
lowed by C–N bond cleavage and hydrolysis delivers product **41-2**.  $\beta$ -F elimination of **41-10** affords product **41-3**. The electrophilic Ni(II) or Mn(II) species promote nucleophilic attack of  $\alpha$ -carbon of acyl to *gem*-difluoroalkene moiety, forming a 5-*endo* cyclization intermediate **41-11**.  $\beta$ -F elimination followed by ring contraction furnishes product **41-4**.

Experimental and DFT calculation studies further support the proposed reaction mechanism ([Scheme 42](#)). The  $\sigma$ -alkyl-Ni(II) complex **42-1** was synthesized and the structure was confirmed by X-ray single crystal diffraction analysis and quenching experiments. Stoichiometric experiments clearly show that  $\sigma$ -alkyl-Ni(II) complex is a key intermediate in the reaction. Control experiments using  $\sigma$ -alkyl-Ni(II) complexes indicate that 1,2-aryl(acyl)/Ni dyotropic rearrangement occurs only when the  $\sigma$ -alkyl-Ni(II) complex **41-5** is reduced to the  $\sigma$ -alkyl-Ni(I) species **41-6**.

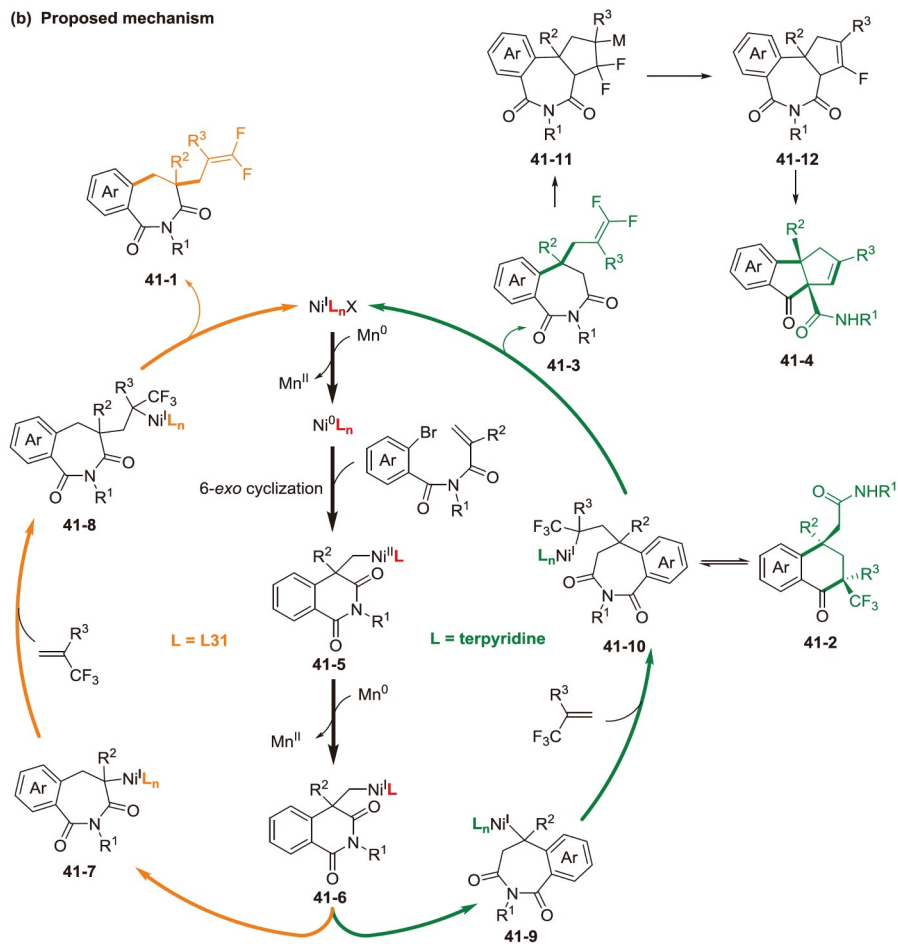
This transformation is of high synthetic value as it represents a conceptually unprecedented new approach to C–C bond activation. This process formally breaks an unactivated C–C  $\sigma$  bond while simultaneously forming a new C–C  $\sigma$  bond and a new C–Ni bond, which can be further functionalized. This strategy can be widely applied in the future to construct complex scaffolds through skeleton rearrangements.

Vinylallenes have been used as key synthons in various metal-catalyzed cycloadditions. In 1998, Murakami and Ito *et al.* [87] reported a Rh-catalyzed intermolecular [4+2] cycloaddition reaction of vinylallenes and alkynes to give the corresponding multi-substituted benzenes. Recently, Arai *et al.* [88] reported a nickel-catalyzed regiodivergent intramolecular [4+2] or [2+2] cycloaddition of vinylallenes and alkynes, leading to the exclusive formation of highly functionalized cyclohexadiene and cyclobutene derivatives ([Scheme 43](#)).

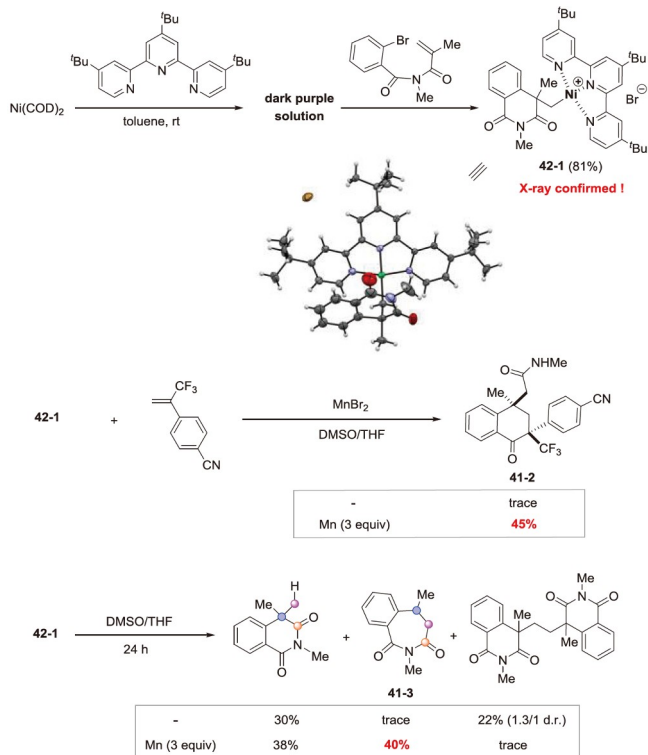
1,6-Enynes had emerged as valuable substrates for hydrosilylation/cyclization reactions constructing silylcyclization products. Rh-catalyzed hydrosilylation/cyclization of 1,6-enynes typically affords vinylsilanes *via* C(sp<sup>2</sup>)–Si bond formation. In 2016, the Lu group [89] reported the first Co-catalyzed hydrosilylation/cyclization of 1,6-enynes, which afforded alkyl silane products. Very recently, the Ge group [90] further developed an asymmetric variant of the cobalt-catalyzed cyclization reactions. Such transformation gave vinyl silanes when alkyl-substituted 1,6-enynes were used, and the alkyl silane products were formed only with aryl-substituted enynes. In 2022, Chang *et al.* [91] reported a divergent nickel-catalyzed hydrosilylation/cyclization of 1,6-enynes. Alkyl silanes **44-1** were obtained in good yields with excellent regioselectivity in the presence of Ni(COD)<sub>2</sub> when THF was used as a solvent. In contrast, when the large steric hindrance ligand IPr was employed, the vinyl silane products **44-2** were produced ([Scheme 44](#)).



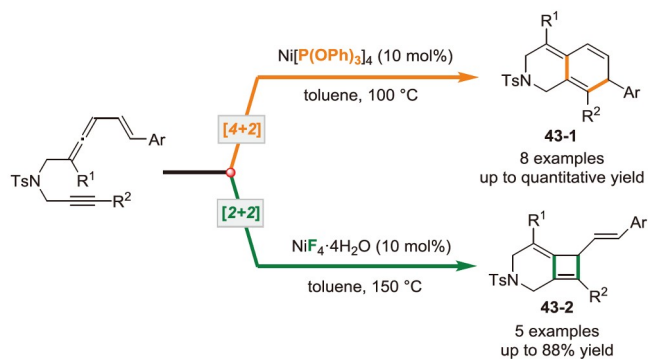
## (b) Proposed mechanism



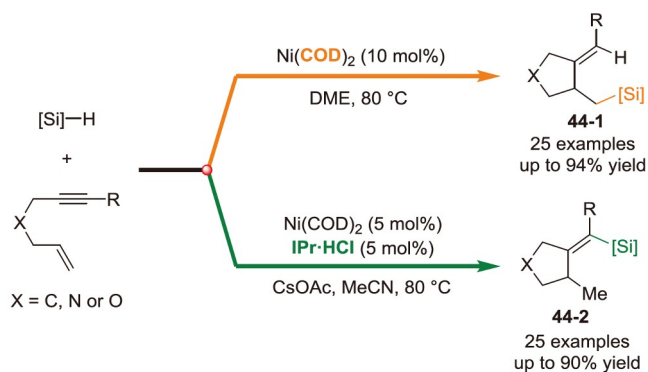
Scheme 41 Ni-catalyzed switchable dyotropic rearrangement [86] (color online).



**Scheme 42** Mechanistic studies of dyotropic rearrangement reaction [86] (color online).



**Scheme 43** Ni-catalyzed regiodivergent [4+2] or [2+2] cycloaddition of vinylallenes and alkynes [88] (color online).



**Scheme 44** Ni-catalyzed regiodivergent hydrosilylation/cyclization of 1,6-enynes and silanes [91] (color online).

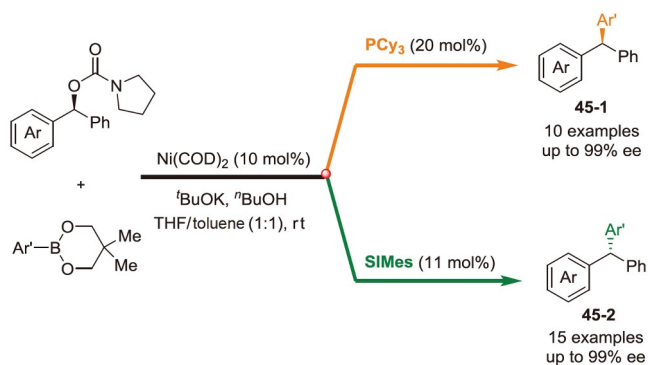
## 4 Stereoselectivity

Stereospecific reactions proceed with inversion or retention, preserving the stereochemical information present in the starting materials without the need for identifying a chiral catalyst. Such reactions are valuable in late-stage synthesis, as they provide a predictable means of constructing stereochemically complex intermediates. In 1990, Hiyama *et al.* [92] demonstrated the first example of Pd-catalyzed couplings of alkylsilanes that could proceed with retention or inversion. Subsequently, the Suginome group [93] developed a stereospecific Suzuki-Miyaura coupling of enantioenriched  $\alpha$ -(acetylamino)benzylboronic esters with aryl bromides, controlled by the choice of additives to selectively afford either retention or inversion. In 2013, Jarvo *et al.* [94] developed a nickel-catalyzed ligand-controlled stereospecific coupling of benzylic carbamates with arylboronic esters. The choice of achiral ligand controls whether the reaction proceeds with inversion or retention at the electrophilic carbon, and therefore, the enantiomer of the product can be formed from a single enantiomer of the starting material. Tricyclohexylphosphine ligand provided the products with retention, while an *N*-heterocyclic carbene ligand provided the products with inversion (Scheme 45).

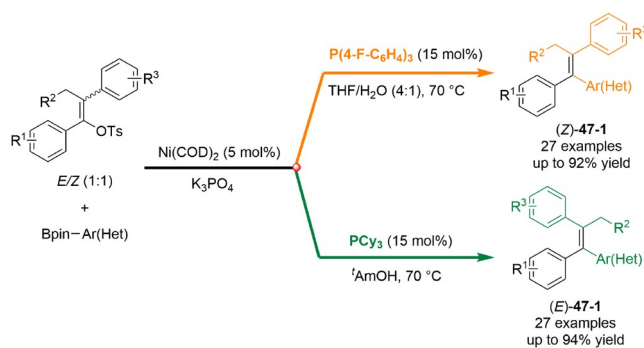
Precise stereocontrolled synthesis of functionalized alkenes is a long-standing research topic in organic synthesis. The development of catalytic, readily tunable synthetic methods for the synthesis of *E*-selective and more challenging *Z*-selective alkenes is extremely challenging. In 2004, Mori *et al.* [95] disclosed Ni-catalyzed ligand-controlled high stereoselective synthesis of *E*- and *Z*-allylsilanes from dienes and aldehydes. *E*-allylsilanes (*E*)-46-1 were selectively formed in the presence of PPh<sub>3</sub> as a ligand. Alternatively, *Z*-allylsilanes (*Z*)-46-1 were selectively formed if a nickel complex with NHC was used for this reaction (Scheme 46a).

A possible reaction mechanism was shown in Scheme 46b. Oxidative cyclization of the diene and the carbonyl group of the aldehyde gives oxanickelacycle 46-4, which is in equilibrium with  $\pi$ -allylnickel complex 46-5.  $\sigma$ -Bond metathesis between 46-5 and hydrosilane followed by reductive elimination gives (*Z*)-46-1. *E*-allylsilane is formed via *syn*- $\pi$ -allylnickelsilane complex 46-2 generated by hydrosilylation of diene.

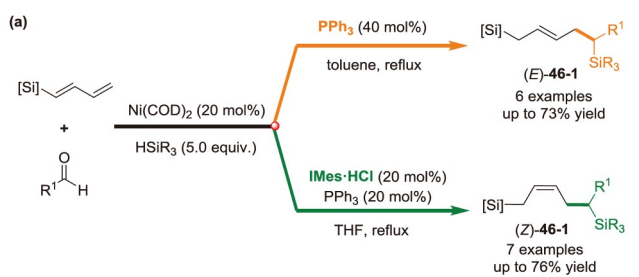
All-carbon tetrasubstituted alkene structural motifs have displayed significant biological activity and found widespread applications in the pharmaceutical industry. However, highly stereoselective methods for the assembly of acyclic tetrasubstituted alkenes have remained scarce. In general, it is accepted that the coupling of stereochemically defined alkenyl halides will preserve the stereochemistry regardless of their original *E*- or *Z*-state. Later studies have found that the ligands coordinated to palladium have a profound effect



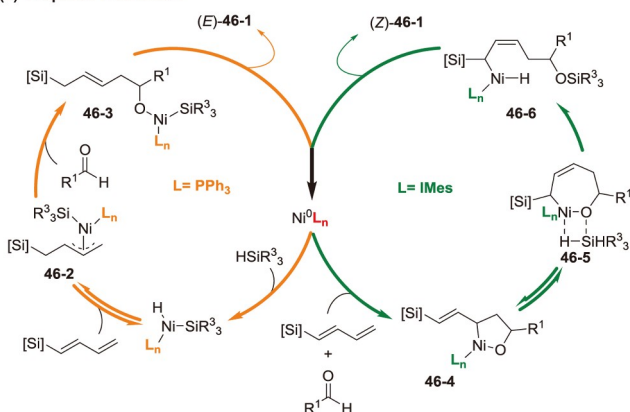
**Scheme 45** Ni-catalyzed ligand-controlled stereospecific cross-coupling of benzylic carbamates with arylboronic esters [94] (color online).



**Scheme 47** Ni-catalyzed stereodivergent cross-coupling reactions of enol tosylates and pinacol boronates [98] (color online).



**(b) Proposed mechanism**



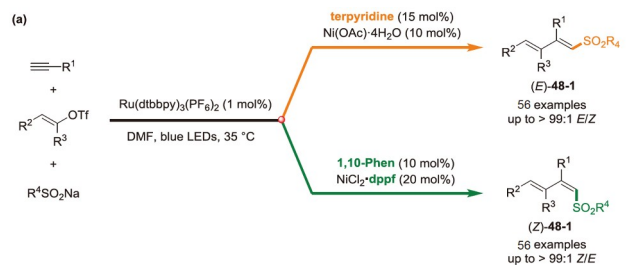
**Scheme 46** Ni-catalyzed ligand-controlled stereodivergent coupling reactions of 1,3-dienes and aldehyde [95] (color online).

on the stereochemical outcome. Lipshutz pioneered the study of Pd-catalyzed stereodivergent cross-coupling of disubstituted alkenyl halides [96,97]. In 2021, the Sigman group [98] reported a method to diastereoselectively access tetrasubstituted alkenes *via* nickel-catalyzed Suzuki-Miyaura cross-couplings of enol tosylates and boronic acid esters. Either diastereomeric product was selectively obtained from a mixture of the enol tosylates diastereomers by simply switching the ligand and solvent system (Scheme 47). It is worth mentioning that the high-throughput ligand screening was performed under the guidance of the Kraken organophosphorus(III) descriptor library. The synthetic utility of the catalytic system was then demonstrated in the stereoselective synthesis of various tetrasubstituted alkenes, with yields up

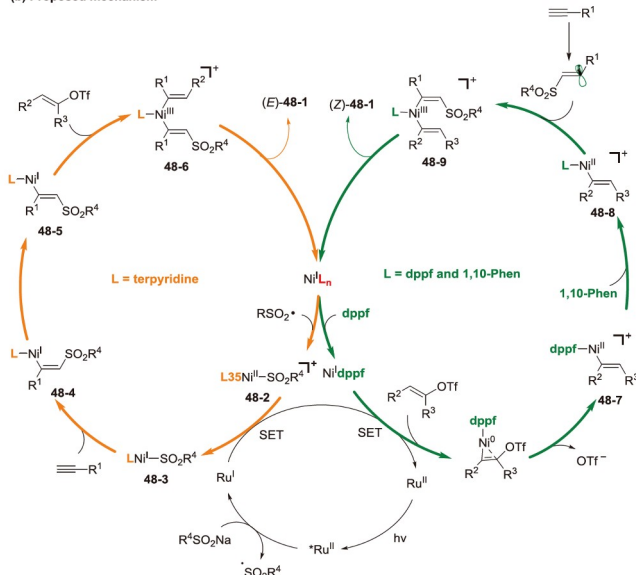
to 94% and diastereomeric ratios up to 99:1 *Z/E* and 93:7 *E/Z* observed.

1,3-Dienes are one of the most important structural motifs commonly found in many natural products and bioactive compounds, as well as serve as valuable building blocks for diverse transformations in synthetic chemistry. However, catalytic stereodivergent strategies that enable the *E*- and *Z*-selective synthesis of substituted 1,3-dienes remain underexploited. Recently, catalytic 1,2-difunctionalization of alkynes *via* dual nickel/photoredox catalysis has been developed to furnish trisubstituted alkenes with anti-selectivity [99–101]. Nevertheless, rare examples of stereodivergent synthesis of both *trans*- and *cis*-substituted alkenes from alkynes have been reported. Very recently, Chu and co-workers [102] demonstrated a ligand-controlled stereodivergent alkenyl-functionalization of alkynes with vinyl triflates and sodium sulfinates *via* photoredox and nickel dual catalysis. With suitable nickel catalysts and ligands, this method enables efficient and divergent access to both *Z*- and *E*-sulfonyl-1,3-dienes from the same starting materials (Scheme 48a).

A possible reaction mechanism was proposed in Scheme 48b. In the case of terpyridine as a ligand, the sulfonyl radical is trapped by Ni(I) to give  $\text{RSO}_2\text{-Ni(II)}$  **48-2**, which is then single-electron reduced by Ru(I) to generate  $\text{RSO}_2\text{-Ni(I)}$  **48-3**. Regioselective migratory insertion of **48-3** into alkyne delivers *cis*-alkenyl Ni(I) species **48-4**, which undergoes isomerization to afford the *trans*-alkenyl Ni(I) **48-5**. Oxidative addition of **48-5** with vinyl triflate affords *trans*-Ni(III) **48-6**, which undergoes reductive elimination to furnish *anti*-addition diene (*E*)-**48-1**. In the case of  $\text{NiCl}_2\text{-dppf/phen}$ , dppf-ligated Ni(I) is more prone to a SET reduction by Ru(I) to generate Ni(0) species, followed by facile oxidative addition with vinyl triflate to form dppf-ligated alkenyl-Ni(II) **48-7**. **48-7** undergoes further ligand exchange with 1,10-phen to form phen-ligated alkenyl-Ni(II) **48-8**. The vinyl radical is generated from the addition of sulfonyl radical to alkyne captured by phen-ligated alkenyl-Ni(II) **48-8** to form the more stable *cis*-Ni(III) species **48-9**, which undergoes



(b) Proposed mechanism

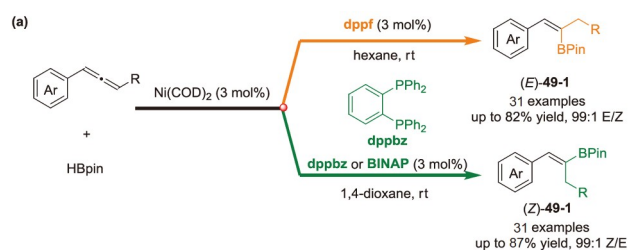


**Scheme 48** Ligand-controlled stereodivergent alkenylation of alkynes with vinyl triflates and sodium sulfonates [102].

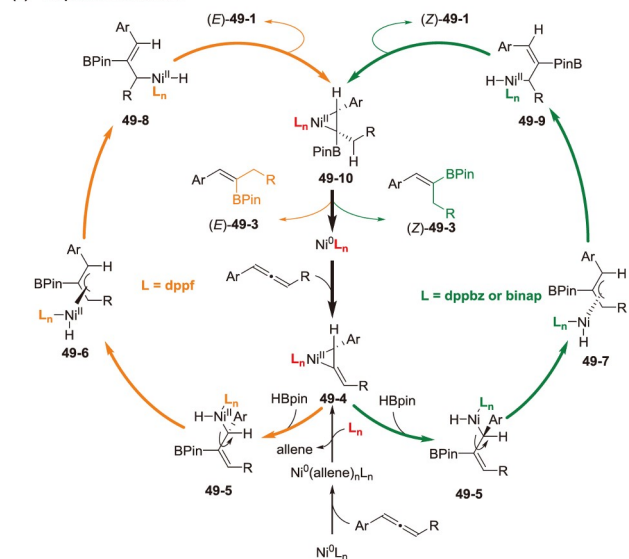
reductive elimination to furnish *syn*-selective product (Z)-48-1.

Transition metal-catalyzed hydroboration of allenes is a well-known process that can produce allylboronate or alkenylboronate compounds. In contrast to the well-established *Z*-stereoselective hydroboration of allenes, examples of *E*-stereoselective hydroboration of allenes are extremely rare. The only example of *E*-stereoselective hydroboration is the copper-catalyzed hydroboration of allene reported by Tsuji *et al.* [103]. Recently, the Ge group [104] developed a convenient and effective protocol for the synthesis of stereo-defined trisubstituted *Z*- and *E*-alkenylboronates through ligand-controlled nickel-catalyzed stereodivergent hydroboration of allenes (Scheme 49a).

DFT calculations were conducted to understand the reaction mechanism (Scheme 49b). The bisphosphine-ligated nickel-allene complex 49-4, formed by the replacement of COD with allenes followed by the coordination of bisphosphine ligands, reacts with HBpin to form the corresponding nickel-olefin complex 49-5, which is the stereo-determining step in these stereodivergent hydroboration reactions. Minimizing the steric interaction between bisphosphine and boryl-containing allyl groups in allylnickel intermediates with maintaining the steric saturation around the nickel



(b) Proposed mechanism



**Scheme 49** Nickel-catalyzed regioselective hydroboration of internal alkenes [104] (color online).

center controls the stereochemistry outcome of alkenylboronate products.

## 5 Conclusions and perspective

In summary, the recent achievements in nickel-catalyzed divergent and selective transformations have been summarized and discussed. By employing different ligands, distinct molecular scaffolds can be selectively obtained from identical starting materials under otherwise almost identical reaction conditions. The strategy does not only lead to scaffolds for library synthesis applications, but could also reveal novel modes of transition-metal catalysis. Despite the significant progress that has been made in this rapidly developing research field over the past few years, many interesting challenges and also opportunities have yet to be addressed.

Although many of the reported ligand-directed divergent catalysis reactions are serendipitous discoveries, careful observation of the effect of ligands on the regioselectivity and chemoselectivity of the reactions, and further optimization of conditions will lead to the discovery of catalytic transformations with broader synthetic utility.

For practical application, strictly catalyst-controlled



selectivities can usually be further improved by traditional approaches such as changes in solvent, temperature, or additives.

Computational methods to visualize and rationalize the transition states governing the selective reactions offer an exciting dimension to improve the understanding and design of selective catalysts.

An increasing number of ligands are being designed, and a wide range of accessible ligand classes provide the necessary tools to discover other catalytic ligand-directed different synthetic applications. Consequently, the development of transition metal-catalyzed ligand-controlled divergent transformations will no doubt be a strong field of investigation for years to come.

**Acknowledgements** This work was supported by the National Natural Science Foundation of China (22171215), Hubei Provincial Outstanding Youth Fund (2022CFA092), and Guangdong Basic and Applied Basic Research Foundation (2022A1515010246).

**Conflict of interest** The authors declare no conflict of interest.

- Frearson JA, Collie IT. *Drug Discov Today*, 2009, 14: 1150–1158
- Macarron R, Banks MN, Bojanic D, Burns DJ, Cirovic DA, Garyantes T, Green DVS, Hertzberg RP, Janzen WP, Paslay JW, Schopfer U, Sittampalam GS. *Nat Rev Drug Discov*, 2011, 10: 188–195
- Ertl P, Jelfs S, Mühlbacher J, Schuffenhauer A, Selzer P. *J Med Chem*, 2006, 49: 4568–4573
- Shelat AA, Guy RK. *Nat Chem Biol*, 2007, 3: 442–446
- O'Connor CJ, Beckmann HSG, Spring DR. *Chem Soc Rev*, 2012, 41: 4444–4456
- Kim J, Kim H, Park SB. *J Am Chem Soc*, 2014, 136: 14629–14638
- Galloway WRJD, Isidro-Llobet A, Spring DR. *Nat Commun*, 2010, 1: 80
- Lee ML, Schneider G. *J Comb Chem*, 2001, 3: 284–289
- Mahatthananchai J, Dumas AM, Bode JW. *Angew Chem Int Ed*, 2012, 51: 10954–10990
- Afagh NA, Yudin AK. *Angew Chem Int Ed*, 2010, 49: 262–310
- Peng JB, Wu XF. *Angew Chem Int Ed*, 2018, 57: 1152–1160
- Garcia-Castro M, Zimmermann S, Sankar MG, Kumar K. *Angew Chem Int Ed*, 2016, 55: 7586–7605
- Lee Y, Kumar K, Waldmann H. *Angew Chem Int Ed*, 2018, 57: 5212–5226
- Chintawar CC, Yadav AK, Kumar A, Sancheti SP, Patil NT. *Chem Rev*, 2021, 121: 8478–8558
- Lee YC, Patil S, Golz C, Strohmman C, Ziegler S, Kumar K, Waldmann H. *Nat Commun*, 2017, 8: 14043
- Beletskaya IP, Nájera C, Yus M. *Chem Soc Rev*, 2020, 49: 7101–7166
- Sakakibara Y, Murakami K. *ACS Catal*, 2022, 12: 1857–1878
- Montgomery J, Savchenko AV. *J Am Chem Soc*, 1996, 118: 2099–2100
- Ikeda S, Yamamoto H, Kondo K, Sato Y. *Organometallics*, 1995, 14: 5015–5016
- Oblinger E, Montgomery J. *J Am Chem Soc*, 1997, 119: 9065–9066
- Yang B, Wang ZX. *J Org Chem*, 2020, 85: 4772–4784
- Li W, Montgomery J. *Chem Commun*, 2012, 48: 1114–1116
- Wiensch EM, Todd DP, Montgomery J. *ACS Catal*, 2017, 7: 5568–5571
- Rand AW, Montgomery J. *Chem Sci*, 2019, 10: 5338–5344
- Lee WC, Shih WC, Wang TH, Liu Y, Yap GPA, Ong TG. *Tetrahedron*, 2015, 71: 4460–4464
- Chen X, Ke H, Zou G. *ACS Catal*, 2014, 4: 379–385
- Entz ED, Russell JEA, Hooker LV, Neufeldt SR. *J Am Chem Soc*, 2020, 142: 15454–15463
- Matsuyama N, Tsurugi H, Satoh T, Miura M. *Adv Synth Catal*, 2008, 350: 2274–2278
- Degtyareva ES, Erokhin KS, Kashin AS, Ananikov VP. *Appl Catal A-Gen*, 2019, 571: 170–179
- Huang Y, Ma C, Liu S, Yang LC, Lan Y, Zhao Y. *Chem*, 2021, 7: 812–826
- Chatupheeraphat A, Liao HH, Srimontree W, Guo L, Minenkov Y, Poater A, Cavallo L, Rueping M. *J Am Chem Soc*, 2018, 140: 3724–3735
- Thane TA, Jarvo ER. *Org Lett*, 2022, 24: 5003–5008
- Seo J, Chui HMP, Heeg MJ, Montgomery J. *J Am Chem Soc*, 1999, 121: 476–477
- Ogoshi S, Nishimura A, Ohashi M. *Org Lett*, 2010, 12: 3450–3452
- Masutomi K, Sakiyama N, Noguchi K, Tanaka K. *Angew Chem Int Ed*, 2012, 51: 13031–13035
- Noucti NN, Alexanian EJ. *Angew Chem Int Ed*, 2013, 52: 8424–8427
- Sakurai H, Imai T. *Chem Lett*, 1975, 4: 891–894
- Takeyama Y, Nozaki K, Matsumoto K, Oshima K, Utimoto K. *BCSJ*, 1991, 64: 1461–1466
- Shintani R, Moriya K, Hayashi T. *Org Lett*, 2012, 14: 2902–2905
- Chen H, Chen Y, Tang X, Liu S, Wang R, Hu T, Gao L, Song Z. *Angew Chem Int Ed*, 2019, 58: 4695–4699
- Wang XC, Li B, Ju CW, Zhao D. *Nat Commun*, 2022, 13: 3392
- Moragas T, Cornella J, Martin R. *J Am Chem Soc*, 2014, 136: 17702–17705
- van Gemmeren M, Börjesson M, Tortajada A, Sun SZ, Okura K, Martin R. *Angew Chem Int Ed*, 2017, 56: 6558–6562
- Gan Y, Xu W, Liu Y. *Org Lett*, 2019, 21: 9652–9657
- Long J, Xia S, Wang T, Cheng GJ, Fang X. *ACS Catal*, 2021, 11: 13880–13890
- Peng L, Li Y, Li Y, Wang W, Pang H, Yin G. *ACS Catal*, 2018, 8: 310–313
- Tortajada A, Menezes Correia JT, Serrano E, Monleón A, Tampieri A, Day CS, Juliá-Hernández F, Martin R. *ACS Catal*, 2021, 11: 10223–10227
- Zhao WT, Meng H, Lin JN, Shu W. *Angew Chem Int Ed*, 2023, 62: e202215779
- Lee WC, Chen CH, Liu CY, Yu MS, Lin YH, Ong TG. *Chem Commun*, 2015, 51: 17104–17107
- Li RP, Shen ZW, Wu QJ, Zhang J, Sun HM. *Org Lett*, 2019, 21: 5055–5058
- Xiao LJ, Cheng L, Feng WM, Li ML, Xie JH, Zhou QL. *Angew Chem Int Ed*, 2018, 57: 461–464
- Li ZQ, Fu Y, Deng R, Tran VT, Gao Y, Liu P, Engle KM. *Angew Chem*, 2020, 132: 23506–23512
- Qian D, Hu X. *Angew Chem Int Ed*, 2019, 58: 18519–18523
- Xue Y, Chen J, Song P, He Y, Zhu S. *Synlett*, 2021, 32: 1647–1651
- Zhao L, Zhu Y, Liu M, Xie L, Liang J, Shi H, Meng X, Chen Z, Han J, Wang C. *Angew Chem Int Ed*, 2022, 61: e202204716
- Xiao J, He Y, Ye F, Zhu S. *Chem*, 2018, 4: 1645–1657
- Zhang Y, He J, Song P, Wang Y, Zhu S. *CCS Chem*, 2020, 2: 2259–2268
- Williams CM, Johnson JB, Rovis T. *J Am Chem Soc*, 2008, 130: 14936–14937
- Seo H, Liu A, Jamison TF. *J Am Chem Soc*, 2017, 139: 13969–13972
- Meng QY, Wang S, Huff GS, König B. *J Am Chem Soc*, 2018, 140: 3198–3201
- Zhang B, Yang S, Li D, Hao M, Chen BZ, Li Z. *ACS Sustain Chem Eng*, 2021, 9: 4091–4101
- Gao J, Jiao M, Ni J, Yu R, Cheng GJ, Fang X. *Angew Chem Int Ed*, 2021, 60: 1883–1890
- Miller KM, Jamison TF. *J Am Chem Soc*, 2004, 126: 15342–15343
- Moslin RM, Jamison TF. *Org Lett*, 2006, 8: 455–458

- 65 Bahadoor AB, Flyer A, Micalizio GC. *J Am Chem Soc*, 2005, 127: 3694–3695
- 66 Jackson EP, Malik HA, Sormunen GJ, Baxter RD, Liu P, Wang H, Shareef AR, Montgomery J. *Acc Chem Res*, 2015, 48: 1736–1745
- 67 Standley EA, Tasker SZ, Jensen KL, Jamison TF. *Acc Chem Res*, 2015, 48: 1503–1514
- 68 Malik HA, Sormunen GJ, Montgomery J. *J Am Chem Soc*, 2010, 132: 6304–6305
- 69 Liu P, Montgomery J, Houk KN. *J Am Chem Soc*, 2011, 133: 6956–6959
- 70 Han LB, Zhang C, Yazawa H, Shimada S. *J Am Chem Soc*, 2004, 126: 5080–5081
- 71 Gao F, Hoveyda AH. *J Am Chem Soc*, 2010, 132: 10961–10963
- 72 Sun F, Yang C, Ni J, Cheng GJ, Fang X. *Org Lett*, 2021, 23: 4045–4050
- 73 Deng HP, Fan XZ, Chen ZH, Xu QH, Wu J. *J Am Chem Soc*, 2017, 139: 13579–13584
- 74 Till NA, Smith RT, MacMillan DWC. *J Am Chem Soc*, 2018, 140: 5701–5705
- 75 Yue H, Zhu C, Kancherla R, Liu F, Rueping M. *Angew Chem Int Ed*, 2020, 59: 5738–5746
- 76 Zhang Y, Tanabe Y, Kuriyama S, Nishibayashi Y. *Chem Eur J*, 2022, 28: e202200727
- 77 Colby EA, O'Brien KC, Jamison TF. *J Am Chem Soc*, 2005, 127: 4297–4307
- 78 Chan J, Jamison TF. *J Am Chem Soc*, 2004, 126: 10682–10691
- 79 Knapp-Reed B, Mahandru GM, Montgomery J. *J Am Chem Soc*, 2005, 127: 13156–13157
- 80 Shareef AR, Sherman DH, Montgomery J. *Chem Sci*, 2012, 3: 892–895
- 81 Tamura R, Yamada Y, Nakao Y, Hiyama T. *Angew Chem Int Ed*, 2012, 51: 5679–5682
- 82 Nakao Y, Idei H, Kanyiva KS, Hiyama T. *J Am Chem Soc*, 2009, 131: 15996–15997
- 83 Donets PA, Cramer N. *Angew Chem Int Ed*, 2015, 54: 633–637
- 84 Pan Q, Ping Y, Wang Y, Guo Y, Kong W. *J Am Chem Soc*, 2021, 143: 10282–10291
- 85 Ping Y, Li X, Pan Q, Kong W. *Angew Chem Int Ed*, 2022, 61: e202201574
- 86 Ping Y, Pan Q, Guo Y, Liu Y, Li X, Wang M, Kong W. *J Am Chem Soc*, 2022, 144: 11626–11637
- 87 Murakami M, Ubukata M, Itami K, Ito Y. *Angew Chem Int Ed*, 1998, 37: 2248–2250
- 88 Arai S, Inagaki S, Nakajima M, Nishida A. *Chem Commun*, 2021, 57: 11268–11271
- 89 Xi T, Lu Z. *J Org Chem*, 2016, 81: 8858–8866
- 90 You Y, Ge S. *Angew Chem Int Ed*, 2021, 60: 12046–12052
- 91 Bai D, Cheng R, Yang J, Xu W, Chen X, Chang J. *Org Chem Front*, 2022, 9: 5285–5291
- 92 Hatanaka Y, Hiyama T. *J Am Chem Soc*, 1990, 112: 7793–7794
- 93 Awano T, Ohmura T, Suginome M. *J Am Chem Soc*, 2011, 133: 20738–20741
- 94 Harris MR, Hanna LE, Greene MA, Moore CE, Jarvo ER. *J Am Chem Soc*, 2013, 135: 3303–3306
- 95 Sawaki R, Sato Y, Mori M. *Org Lett*, 2004, 6: 1131–1133
- 96 Krasovskiy A, Lipshutz BH. *Org Lett*, 2011, 13: 3818–3821
- 97 Lu GP, Voigttritter KR, Cai C, Lipshutz BH. *J Org Chem*, 2012, 77: 3700–3703
- 98 Zell D, Kingston C, Jermaks J, Smith SR, Seeger N, Wassmer J, Sirois LE, Han C, Zhang H, Sigman MS, Gosselin F. *J Am Chem Soc*, 2021, 143: 19078–19090
- 99 Li Z, García-Domínguez A, Nevado C. *Angew Chem Int Ed*, 2016, 55: 6938–6941
- 100 Jiang Y, Pan J, Yang T, Zhao Y, Koh MJ. *Chem*, 2021, 7: 993–1005
- 101 Zhu C, Yue H, Maity B, Atodiresi I, Cavallo L, Rueping M. *Nat Catal*, 2019, 2: 678–687
- 102 Long T, Zhu C, Li L, Shao L, Zhu S, Rueping M, Chu L. *Nat Commun*, 2023, 14: 55
- 103 Semba K, Shinomiya M, Fujihara T, Terao J, Tsuji Y. *Chem Eur J*, 2013, 19: 7125–7132
- 104 Yang X, Yuan C, Ge S. *Chem*, 2023, 9: 198–215